RESEARCH ARTICLE

Improved effectiveness of vaccination campaigns against rabies by reducing spatial heterogeneity in coverage

Elaine A. Ferguson[1]*, Ahmed Lugelo[2,3], Anna Czupryna[1], Danni Anderson[1], Felix Lankester[3,4], Lwitiko Sikana[2], Jonathan Dushoff[5], Katie Hampson[1]

1 Boyd Orr Centre for Population and Ecosystem Health, School of Biodiversity, One Health & Veterinary Medicine, College of Medical, Veterinary & Life Sciences, University of Glasgow, Glasgow, United Kingdom, 2 Environmental Health and Ecological Sciences Department, Ifakara Health Institute, Ifakara, Tanzania, 3 Global Animal Health Tanzania, Arusha, Tanzania, 4 Paul G. Allen School for Global Health, Washington State University, Pullman, Washington, United States of America, 5 Department of Biology, McMaster University, Hamilton, Ontario, Canada

* Elaine.Ferguson@glasgow.ac.uk

Abstract

Vaccination programs are the mainstay of control for many infectious diseases. Heterogeneous coverage is hypothesized to reduce vaccination program effectiveness, but this impact has not been quantified in real systems. We address this gap using fine-scale data from two decades of rabies contact tracing and dog vaccination campaigns in Serengeti district, Tanzania. We also aimed to identify drivers of the continued circulation of rabies in the district despite annual vaccination campaigns. Using generalized linear mixed models, we find that current focal (village-level) dog rabies incidence decreases with increasing recent focal vaccination coverage. However, current focal incidence depends most on recent incidence, both focally and in the wider district, consistent with high population connectivity. Removing the masking effects of prior non-focal incidence shows that, for the same average prior non-focal (wider-district) vaccination coverage, increased heterogeneity in coverage among the non-focal villages leads to increased focal incidence. These effects led to outbreaks following years when vaccination campaigns missed many villages, whereas when heterogeneity in coverage was reduced, incidence declined to low levels (<0.4 cases/1,000 dogs annually and no human deaths) and short vaccination lapses thereafter did not lead to resurgence. Through transmission-tree reconstruction, we inferred frequent incursions into the district each year (mean of 7). Inferred incursions substantially increased as a percentage of all cases in recent years, reaching 50% in 2022, suggesting regional connectivity is driving residual transmission. Overall, we empirically demonstrate how population connectivity and spatial heterogeneity in vaccination can impact disease outcomes, highlighting the importance of fine-scale monitoring in managing vaccination programs.

Introduction

Vaccination of domestic dogs to interrupt rabies transmission is a quintessential One Health intervention that mitigates risks of human infection from this fatal zoonotic disease [1,2]. While the impacts of vaccinating human populations against childhood diseases have been studied extensively, vaccination of animal populations has not been examined in the same detail, and impacts may differ for a number of reasons. Firstly, demographic turnover and therefore waning of vaccine-induced immunity is likely to be faster in many animal populations than in humans [3–5]; secondly, with the exception of species that undertake long-range migrations [6], animal movement is often more local, perhaps curtailing the geographic spread of disease [7]; and thirdly, vaccinating animals is potentially more difficult, with logistical challenges resulting in lower and/or more heterogeneous coverage [8–11]. Moreover, understanding how vaccination coverage impacts transmission in animal populations could have far-reaching implications for a range of zoonoses and for diseases that threaten food security and endangered wildlife.

The implications of the specific challenges of animal vaccination are important to understand for rabies, a fatal but vaccine-preventable viral disease of mammals. Rabies kills tens of thousands of people every year and causes billions of dollars of economic losses [12], with dog-mediated rabies being the cause of >99% of human rabies deaths [13]. Human post-exposure vaccines are effective in preventing infection onset, but are costly for both the health sector and bite victims, and lack of access to these emergency vaccines has tragic consequences [14–16]. However, rabies can be tackled at source through mass dog vaccination. When sufficient coverage is reached, dog vaccination can interrupt transmission and even eliminate rabies, with economic benefits from the reduced need for post-exposure vaccines [17–19]. Dog vaccination is therefore the cornerstone of the global strategic plan, 'Zero by 30', to end human deaths from dog-mediated rabies by 2030 [20].

Rabies control by mass dog vaccination is not a new concept. Dog vaccination was integral to the elimination of rabies from Japan in 1957, and is still maintained as a safeguard against reintroductions [21]. Mass dog vaccination was also central to reducing dog-mediated rabies by >95% between 1980 and 2010 in Latin America and the Caribbean [22], with Mexico becoming the first country validated by WHO as free from dog-mediated human rabies since the 'Zero by 30' initiative began [23]. Despite these huge strides in the Americas, mass dog vaccination has not been implemented at scale across Africa and Asia. Pilot vaccination projects have reduced local rabies incidence [24–27], dispelled doubts about the accessibility of free-roaming dogs for vaccination, elucidated their role as the reservoir population [28], and provided valuable lessons for improving vaccination campaign design [29–31]. However, piecemeal vaccination efforts are not often maintained or rolled out nationally due to low prioritization of this neglected disease [32]. Lack of consistent, large-scale vaccination may have negative consequences for the long-term impacts of local efforts. Areas where rabies has been eliminated, but where dog vaccination has lapsed, are vulnerable to reintroductions, as observed in many settings [26,33,34]. However, relatively little is known about rates of incursions and

the distances over which they can penetrate into control areas. Better understanding of incursion risks would inform, for example, how wide vaccinated buffer zones must be to prevent introductions from establishing. Further knowledge of how incursions, local dog movements, and vaccination efforts interact to drive disease dynamics would also provide valuable guidance to rabies-endemic countries as they develop strategic plans to reach the 'Zero by 30' goal.

Assessments of mass dog vaccination campaigns suggest that coverage can be highly heterogeneous [29,35,36], often failing to reach the recommended 70% target [25,37]. Reasons for these outcomes include lack of resources and insufficient attention to barriers affecting participation [9,10,35]. This is concerning, as simulation-based models indicate that patches of low coverage could jeopardize rabies control more widely [36,38]. However, the impacts of heterogeneous coverage have rarely, if ever, been quantified using incidence data from a real animal or human system, rabies or otherwise. Fine-scale heterogeneities in vaccination coverage may be masked by data aggregated to administrative scales. Such aggregation has been a feature of most empirical studies reporting impacts of rabies vaccination [25,26,39,40] and limits our understanding of how incidence is driven by influences at both local and wider scales. Fine-scale data could allow quantification of these impacts, revealing the consequences of coverage heterogeneities and the extent of epidemiological connectivity.

Here we examine dog rabies and human rabies exposures and deaths in the Serengeti district of northern Tanzania, where dog vaccination has been ongoing since 2003, along with contact tracing to track rabies transmission. It is unclear how rabies has been able to persist in Serengeti district despite control efforts, and in this study, we explore evidence for three hypotheses:

(1) Spatial heterogeneity in vaccination within the district allows rabies to persist in patches of lower coverage;

(2) The mean vaccination coverage over the district has simply been insufficient;

(3) Incursions of rabies from outside the district maintain transmission.

Using contact tracing and vaccination campaign data at fine spatiotemporal scales to inform statistical models, we decipher the cross-scale drivers of viral circulation and draw conclusions on what is necessary to eliminate rabies from an animal reservoir in a connected landscape.

Results

Study area and dog population

Serengeti district consists of 88 villages, each of which shares borders with a median of 5 (range: 2–9) neighboring villages. Village polygons ranged in area from 5.5 to 386.2 km^2, but numbers of cells within these polygons on a 1 km^2 grid (Fig 1A) with a non-zero population (from a georeferenced district-wide census of humans and dogs) ranged from 5 to just 85. The district is bordered both by three other districts within Mara region where rabies circulates endemically, and by Serengeti National Park where domestic dogs are not permitted (Fig 1A).

Serengeti district's human population grew from an estimated 175,017 to 345,587 between January 2002 and December 2022 based on national census data; an average growth rate of 3.2% per annum. Human:dog ratios (estimated from the georeferenced human and dog census) varied from 2.4 to 9.1 between villages (Fig 1C) [42]. The district dog population, estimated from these ratios, approximately doubled over the study period, increasing from 42,931 to 85,672 (Fig 1B). Estimated dog densities in December 2022 ranged from 0 to 625 dogs/km^2 across a 1 km^2 grid (Fig 1A, mean of 21 dogs/km^2 or 37 dogs/km^2 when considering only the 57% of cells with a non-zero dog population). Village-level dog densities, which ranged from 10 to 297 dogs/km^2 in December 2022 (Fig 1D), were calculated by dividing estimated village dog populations by the number of 1 km^2 cells with non-zero population in the village, to better reflect densities experienced by populations in villages with large unoccupied areas, particularly on the North and South borders (Fig 1A).
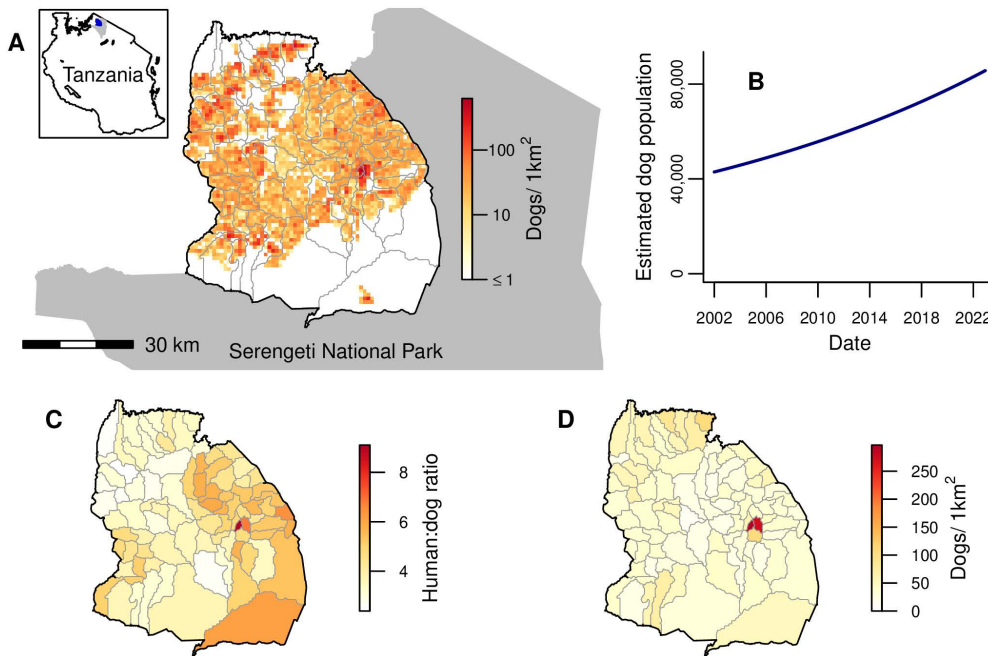
Fig 1. Study area and dog population. (A) Serengeti District bordered by Serengeti National Park (grey shading). Grey lines show village borders within the district. The spatial distribution of the estimated dog population on a 1 km² grid at the end of 2022 is indicated by the color scale (on a log scale). The inset indicates the location of Serengeti District (blue) and Serengeti National Park (grey) within Tanzania. **(B)** Total dog population in Serengeti District from 2002 to 2022, estimated based on national human census data and human:dog ratios. **(C)** Human:dog ratios for each village from a district-wide census of humans and dogs. **(D)** Village-level dog density at the end of 2022, estimated by dividing the estimated village dog populations by the total number of 1 km² cells with non-zero population in each village. Map of Tanzania downloaded at https://www.nbs.go.tz/statistics/topic/gis and Serengeti National Park at https://www.arcgis.com/home/item.html?id=780c707de03842a98a365c30ceef1a74. Map of Serengeti villages developed by [41] and available at https://doi.org/10.5281/zenodo.6308051. The data underlying this figure can be found at https://doi.org/10.5281/zenodo.15012106.

https://doi.org/10.1371/journal.pbio.3002872.g001

Heterogeneous vaccination coverage

Annual rabies vaccination campaigns were initiated as part of a research project in 2003 (Fig 2A) in the district's villages within 10 km of the Serengeti National Park [43,44]. The percentage of villages that held campaigns in 2003, hereafter "campaign completeness", was 48% (Fig 2A, 2E, S1 Table). In 2004, in response to a rabies outbreak [45], campaigns were expanded by the local government, resulting in a campaign completeness of 90% (Fig 2A, 2D–2E). Subsequently, campaigns continued in villages bordering the National Park, and less consistently across the rest of the district, depending on local government resources. Following a resurgence of rabies in 2010–2012, the local government committed to the goal of conducting campaigns annually in all villages throughout the district. Campaign completeness increased gradually, reaching ≥95% throughout 2015–2017. In 2018, vaccination in the northwest villages lapsed again due to logistical constraints (Fig 2A, 2E). But, in 2019, for the first time, campaign completeness reached 100%. In 2021, vaccination did not take place in the southeastern villages for the first time since 2003, however as the 2020 campaigns in these villages happened late in the calendar year and the 2022 campaigns were early, the inter-campaign interval was only 16–18 months. The mean campaign completeness overall years from 2003 to 2022 was 77% of villages/year.

Numbers of dogs vaccinated in campaigns each year ranged from 4,199 in 2003 to 26,419 in 2017 (Fig 2B). Like campaign completeness, dogs vaccinated steadily increased each year following the local government commitment to annual campaigns. However, since the peak in 2017, numbers of dogs vaccinated each year have fallen again, despite the increasing dog population (Fig 2B).
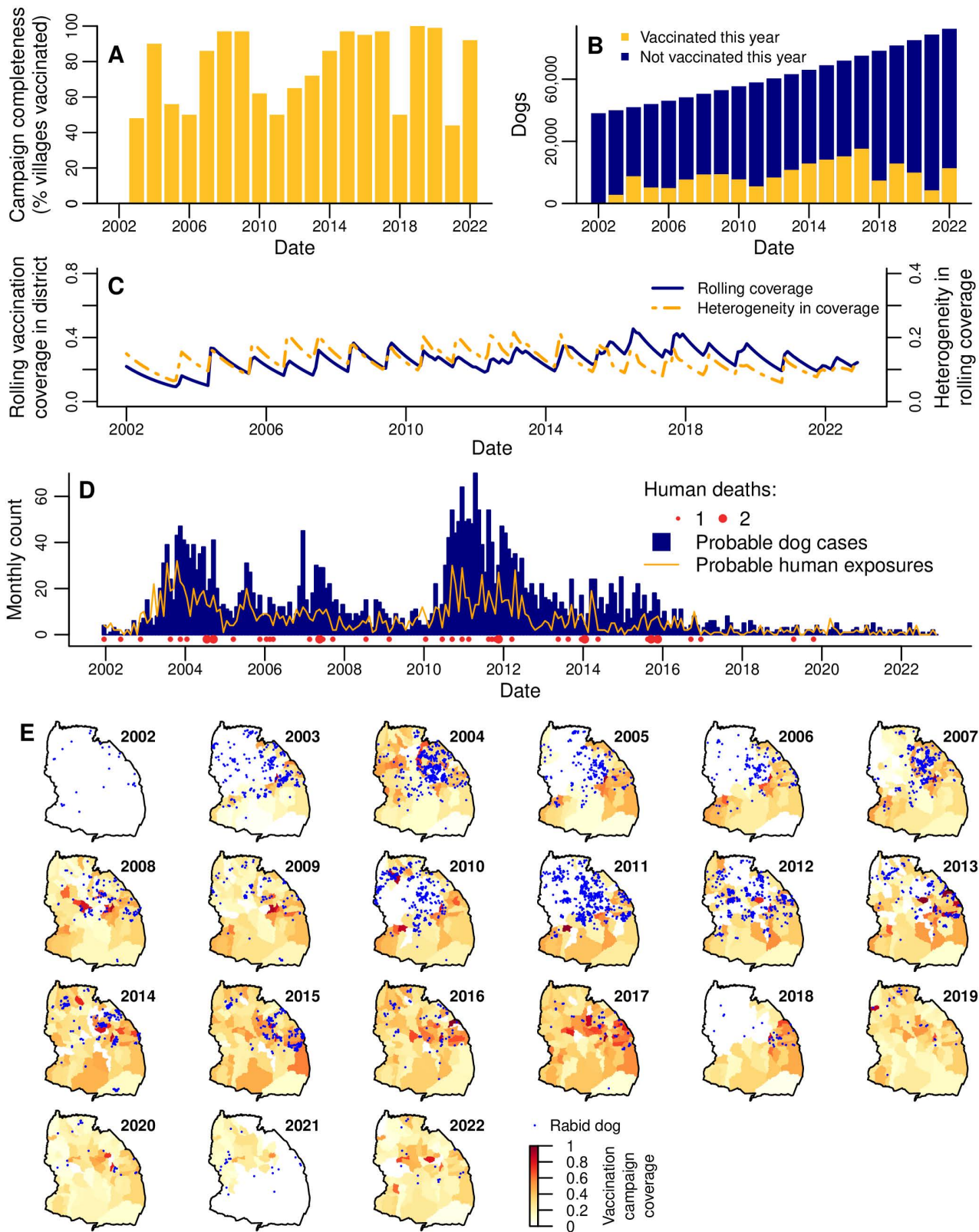
Fig 2. Dog vaccination, dog rabies cases and human rabies exposures and deaths in Serengeti district from 2002 to 2022. (A) Campaign completeness (% villages in the district that held vaccinations) each year. **(B)** Number of dogs that were and were not vaccinated in the district each year.

(C) Monthly district-level 'rolling' dog vaccination coverage (blue line), and monthly heterogeneity in rolling coverage (the population-weighted standard deviation of rolling coverage over all villages in the district; orange line). **(D)** Monthly dog cases, human exposures, and human deaths in the district. **(E)** Village-level 'campaign' vaccination coverage (color scale) and locations of dog rabies cases (blue points) each year (see S1B Fig for campaign coverage maps without overlaid cases). Map of Serengeti villages developed by [41] and available at https://doi.org/10.5281/zenodo.6308051. The data underlying this figure can be found at https://doi.org/10.5281/zenodo.15012106.

From 2003 until 2022, the estimated percentage of dogs vaccinated during annual campaigns (hereafter "campaign coverage") in the district ranged from 8% to 37%, with a mean of 22% of dogs vaccinated per year (S1A Fig, S1 Table). Campaign coverage varied more across villages, from 0.3% to 98%, with a mean of 31% over all annual village-campaigns (Fig 2E). Only 3% of village-campaigns reached the recommended target coverage of 70%.

In each month in 2002–2022, we also estimated the proportion of dogs in the population that had been vaccinated at least once in their lives, accounting for vaccination campaign timing and dog population turnover. This "rolling coverage" estimate can exceed campaign coverage, since it includes vaccinated dogs that have survived from previous years but that may not have been re-vaccinated in the current year (we assume that previously vaccinated and unvaccinated dogs have an equal probability of being vaccinated in annual campaigns). Our estimate of monthly district-level rolling coverage in January 2002 when the study started was 22% based on information from the 2000 to 2001 vaccination campaign preceding our study [25], with subsequent fluctuation between 9% and 45% (mean of 26% over all months; Fig 2B). For most of the study period, there was relatively little variation in the magnitude of district-level rolling coverage (Figs 2B, S2A), but rolling coverage between villages was more variable (S1 Video, S2 Fig). Specifically, coverage heterogeneity, calculated as the standard deviation of rolling coverage over all villages, weighted by village dog populations (Fig 2B), was observed to be higher in 2007 and 2011–2013 (Figs 2C, S2B). The peaks in heterogeneity followed multi-year periods (in 2002–2003, 2005–2006 and 2010–2012) where groups of villages in the northwest were not vaccinated. Single years where groups of villages were not vaccinated (in 2018 and 2021) did not lead to visually obvious drops in the yearly average rolling coverage in those areas (S2C Fig), and this is reflected in relatively low levels of coverage heterogeneity from 2019 to 2022 (Figs 2C, S2B).

Rabies cases and exposures

A total of 3,362 probable dog rabies cases were identified from January 2002 to December 2022 via contact tracing. Identification of probable animal cases was based on the presence of clinical signs along with either: (1) disappearance or death of the animal within 10 days, or (2) the animal being killed and either of unknown origin or known to have previously been bitten [45]. Annually, probable case numbers varied from just 16 (0.19 cases/1,000 dogs) in 2022 up to 547 (9.4 cases/1,000 dogs) in 2011, while monthly cases ranged from 0 to 70 (Fig 2D), never exceeding 17 in any village (S1 Video). Dog cases occurred primarily in the central and northern villages, and were less frequent in the south (Fig 2E). At least one case was recorded in every village, except for two neighboring villages in the west of the district. Dog rabies incidence was relatively low in 2002 but increased over 2003, leading to an outbreak that was largely controlled by the district-wide vaccination campaign in 2004 (Fig 2D–2E). Further outbreaks (which we define as surges with cases exceeding 4/1,000 dogs/year, since this captures the most prominent peaks observed in the district time series) occurred in 2005 and 2007, during or following years without district-wide vaccination and culminated in the largest outbreak from 2010 to 2012. Cases steadily declined from 2012 and remained at low levels of <30 per year (<0.4 cases/1,000 dogs) from 2018 onwards despite lapses in vaccination campaigns in 2018 and 2021 (Fig 2).

Probable human rabies exposures (individuals identified through contact tracing – via bite patient records from health facilities and subsequent interviews with patients/dog-owners – who received a bite/scratch from a probable rabies case) roughly tracked dog rabies, ranging from 0 to 32 exposures per month and peaking in late 2003 (Fig 2D). Annual exposures ranged from 204 in 2003 (111 exposures/100,000 people) to just 11 in 2021 and 2022 (3 exposures/100,000 people), having declined and remained low (≤21 per year) since 2017.

Individual rabid dogs exposed between 0 and 18 people (mean = 0.39; S3 Fig), with 72% exposing no one, and 21% exposing only one person. Of all human exposures, 87.5% were due to domestic dogs. Exposures from other species followed a similar temporal pattern to those by dogs (S4 Fig). Of non-dog-mediated human exposures where the biting species was known, 47.9% were by domestic cats, 18.9% by jackals, 11.6% by livestock, 2.1% by humans, and the remaining 19.5% by various other wildlife species. In comparison, 84.6% of rabid animals identified by contact tracing were domestic dogs, with the remainder being composed of 60.5% livestock, 13.3% domestic cats, 12.0% jackals and 14.1% various other wildlife species.

Overall, 48 human rabies deaths were identified (Fig 2D, S1 Video), with a peak of seven in 2011 (annual incidence of 3 deaths/100,000). Deaths were recorded every year until 2018. Two deaths were recorded again in 2019 despite low numbers of exposures and dog cases, but there were no deaths thereafter. Of the 48 deaths, none completed a full course of post-exposure vaccinations: 3 individuals received one vaccination, 4 received two, and the remaining 41 received none.

Drivers of disease incidence

To understand the drivers of these rabies incidence patterns we used negative binomial generalized linear mixed models (GLMMs). We modelled focal incidence in the current month (monthly cases/dog, i.e., cases in a village each month, with the logged village dog population as an offset) in response to prior rolling vaccination coverage and prior incidence (cases/dog), with a random effect of village. Both prior rolling coverage and prior incidence were included as averages over the previous two months, since >90% of rabies incubation periods recorded during contact tracing were shorter than two months (Fig 2B). Prior rolling coverage and incidence were also considered at three spatial scales: (1) the focal village; (2) bordering villages; and (3) non-bordering villages in the district. We fitted models where prior rolling coverages in bordering and non-bordering villages were incorporated as either arithmetic means of rolling coverage or power means of susceptibility (i.e., 1 − rolling coverage) over those villages. Taking the power mean of susceptibility gives a measure of 'effective susceptibility': the susceptibility of the population to infection, taking into account that the potential for disease spread may depend on both the absolute proportion of susceptible individuals and their spatial distribution, i.e., two populations with the same proportion of susceptible *individuals* may *as populations* differ in vulnerability to disease. In our models, effective susceptibility is adjusted up or down from a simple arithmetic mean susceptibility over villages based on the degree of heterogeneity in susceptibility among those villages and the value of the parameter p (Equation 14), which is fitted as part of our Bayesian inference framework. If $p > 1$, the power mean is biased towards higher susceptibility villages and rises above the arithmetic mean; i.e., for the same total number of unvaccinated dogs, the effective susceptibility is higher when those dogs are distributed unevenly. At $p < 1$, heterogeneity reduces effective susceptibility, and at $p = 1$, we revert to an arithmetic mean model. Since prior incidence at each spatial scale is expected to be partially determined by coverage/susceptibility at that scale (leading to correlation between these variables), including both variables in the model is expected to lead to partial masking of the vaccination effect. To better quantify the full independent impact of vaccination, we therefore fitted versions of the models both with and without the effects of prior incidence at each spatial scale (as specified in Table 1).

Current focal incidence decreased with increasing prior focal rolling coverage (Fig 3A, Table 1, S5A Fig). In the arithmetic mean rolling coverage model with prior incidence, a 10% prior coverage increase in the focal village was associated with a focal incidence decrease of 8.3% (95% credible interval (CrI): 3.2%–13.3%). In the arithmetic mean rolling coverage model without prior incidence, the estimated impact of a 10% increase in prior focal coverage was larger, causing a 13.4% (95% CrI: 8.3%–18.2%) reduction in focal incidence. An impact of prior arithmetic mean rolling coverage in bordering villages was only evident in the model without prior incidence, while an effect of rolling coverage in non-bordering villages was not detected in either arithmetic mean rolling coverage model (Table 1, Figs 3A, S5A).

Table 1. Parameter estimates and WAIC for monthly GLMMs for cases/dog in a focal village in the current month.

Coefficient	1. Arithmetic mean rolling coverage model	2. Arithmetic mean rolling coverage model without prior incidence	3. Power mean susceptibility model	4. Power mean susceptibility model without prior incidence beyond focal village	5. Power mean susceptibility model without prior incidence at any scale
Intercept	−0.28 (−1.16, 0.63)	−1.27 (−2.87, 0.43)	−2.08 (−3.56, −0.61)	−8.67 (−10.74, −6.48)	−12.21 (−14.63, −9.66)
Rolling vaccination coverage in focal village	−0.87 (−1.43, −0.33)*	−1.29 (−1.9, −0.68)*			
Rolling vaccination coverage at borders	−0.27 (−1.06, 0.54)	−1.15 (−2.07, −0.22)*			
Rolling vaccination coverage in non-neighboring villages	−0.37 (−1.41, 0.67)	0.33 (−0.84, 1.51)			
Susceptibility in focal village			0.83 (0.27, 1.37)*	0.27 (−0.27, 0.81)	0.36 (−0.22, 0.93)
Susceptibility at borders			0.32 (−0.53, 1.18)	1.14 (0.23, 2.03)*	1.72 (0.72, 2.69)*
Susceptibility in non-neighboring villages			0.59 (−0.56, 1.83)	5.16 (3.6, 6.68)*	6.43 (4.76, 8.17)*
Log cases/dog in focal village	0.23 (0.21, 0.25)*		0.23 (0.21, 0.25)*	0.29 (0.27, 0.3)*	
Log cases/dog at borders	0.14 (0.11, 0.16)*		0.14 (0.11, 0.16)*		
Log cases/dog in non-neighboring villages	0.4 (0.35, 0.46)*		0.4 (0.34, 0.46)*		
Log dogs/km^2	−0.69 (−0.95, −0.44)*	−2.89 (−3.28, −2.5)*	−0.67 (−0.94, −0.42)*	−1.17 (−1.53, −0.85)*	−1.71 (−2.11, −1.31)*
Human:dog ratio	0.33 (0.19, 0.46)*	0.55 (0.24, 0.84)*	0.33 (0.19, 0.46)*	0.33 (0.18, 0.49)*	0.44 (0.22, 0.67)*
Village random effect standard deviation	0.68 (0.54, 0.83)	1.69 (1.39, 2.05)	0.67 (0.54, 0.83)	0.82 (0.64, 1.04)	1.23 (1, 1.51)
Size (negative binomial distribution parameter)	0.34 (0.3, 0.37)	0.16 (0.15, 0.18)	0.34 (0.3, 0.37)	0.29 (0.26, 0.32)	0.16 (0.15, 0.18)
p (power used in calculating power means)			2.56 (−1.26, 6.19)	10.54 (8.07, 13.22)	12.11 (9.64, 14.67)
WAIC	14,387 (SE: 275)	15,708 (SE: 290)	14,344 (SE: 274)	14,718 (SE: 280)	15,601 (SE: 290)

Ninety-five percent credible intervals (CrIs) in brackets, except for WAIC, where the standard error is provided. Coefficients for fixed effects where the 95% CrI does not include zero are marked *. Model 1 is presented in Fig 3, model 2 in S3 Fig, and models 3 and 4 in Fig 4. Vaccination, susceptibility and cases/dog variables are all averages over the prior two months.

https://doi.org/10.1371/journal.pbio.3002872.t001

We find that incidence increases with power mean susceptibility in bordering and non-bordering villages only when prior incidence at those scales is not included (Table 1, Fig 4A). In those models we estimate p to be substantially larger than one (Table 1, Fig 4B) and beyond what we a priori expected to be the feasible range (S6 Fig). The increase in effective susceptibility at the district level due to heterogeneity (Figs 4C, S8) follows a similar pattern to the standard deviation in village coverage (Figs 2B, S2B), having peaks in 2007 and 2013, and being lower from 2019. The power mean susceptibility model without prior incidence beyond the focal village predicts, for example, that if half the bordering and non-bordering villages had prior coverage of 30%, with the other half having 50%, then the focal village incidence would be 1.4 (95% CrI: 1.3–1.6) times greater than if prior coverage had been homogeneous at 40%. If we further increase heterogeneity by assuming half the villages had prior 20% coverage and the other half 60%, then focal incidence is expected to be 2.6 (95% CrI: 1.9–3.4) times the homogeneous scenario.

Increased prior incidence across all three scales (the focal village, bordering villages, and non-bordering villages) was associated with increased focal incidence (Figs 3A–3B, 5A) and had a greater impact than prior coverage or susceptibility
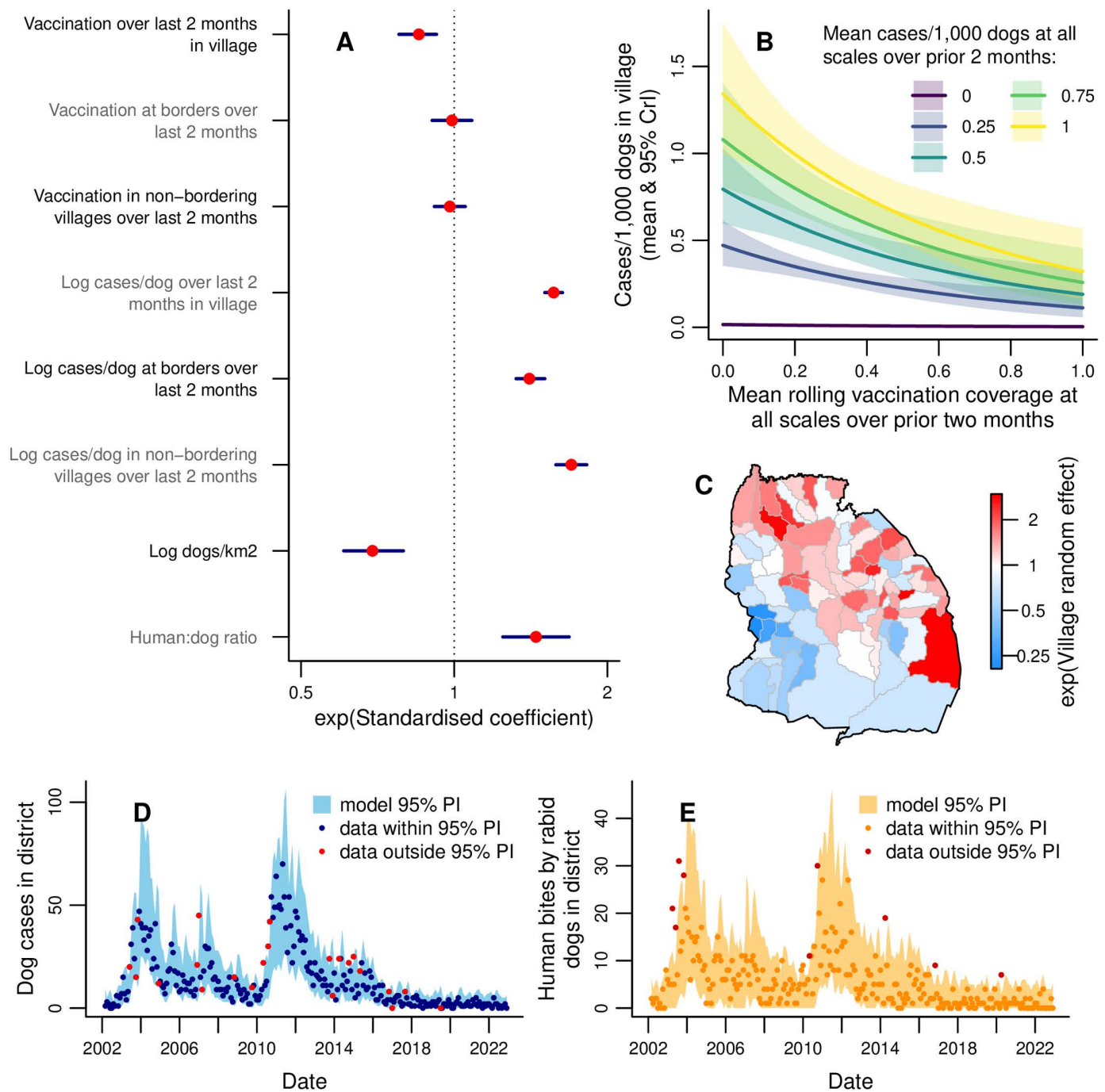
Fig 3. Modelling monthly dog rabies cases in villages. (A) Exponentiated standardized values of the coefficients estimated for each explanatory variable, with 95% credible intervals (CrIs). See Table 1 for tabulated non-standardized parameter values. **(B)** Expected cases/1,000 dogs (number of dog cases normalized by dog population) in a village this month for different mean rolling vaccination coverages and mean cases/dog in the prior 2 months. Prior cases/dog values were chosen to represent the range observed at district level and shaded areas show 95% CrIs, with predictions obtained using average values of unspecified explanatory variables. **(C)** Exponentiated random effect values for each village. **(D)** Comparison of observed monthly dog cases (points) with the 95% prediction interval from the fitted model. **(E)** Human rabies exposures each month (points), with 95% prediction interval from the dog case predictions in **D** and the fitted distribution of exposures per dog (S11 Fig). Data points in red **(D, E)** fall outside the model 95% prediction interval (PI). Map of Serengeti villages developed by [41] and available at https://doi.org/10.5281/zenodo.6308051. The data underlying this figure can be found at https://doi.org/10.5281/zenodo.15012106.

https://doi.org/10.1371/journal.pbio.3002872.g003
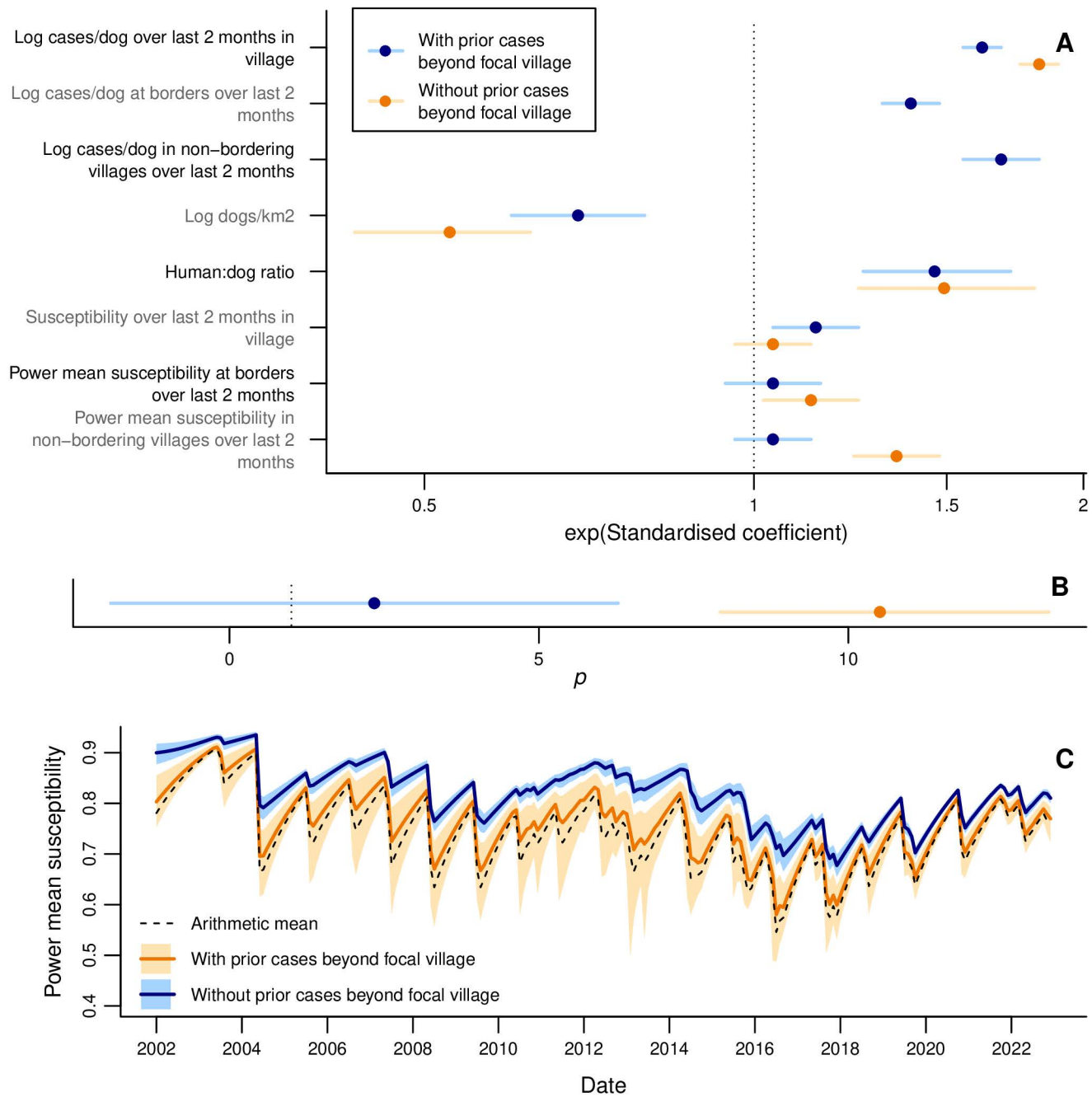
Fig 4. Using power mean susceptibility to model impacts of heterogeneity in vaccination on rabies incidence at the village level. (A) Exponentiated standardized estimated coefficients for explanatory variables, with 95% CrIs. **(B)** Estimated power p used to calculate power mean susceptibilities. **A–B** show estimates from models with (blue) and without (orange) effects of prior incidence beyond the focal village. See Table 1 for tabulated non-standardized parameter values. **(C)** Monthly arithmetic mean susceptibility over all villages in the district, compared with power mean susceptibility (mean and 95% CrI) from fitted values of p from models with and without prior incidence beyond the focal village. The data underlying this video can be found at https://doi.org/10.5281/zenodo.15012106.

https://doi.org/10.1371/journal.pbio.3002872.g004

(Figs 3A, 5A), based on the standardized coefficients (found by transforming all explanatory variables to have a variance of one). Logging the prior incidence explanatory variables improved the fit based on the widely applicable information criterion (WAIC), a Bayesian model selection statistic [46]. Prior incidence in bordering villages had less impact on current focal incidence than prior incidence in non-bordering villages (Figs 3A, 5A). In the arithmetic mean rolling coverage model, doubling mean cases/dog in the focal village over the prior two months led to a 17.3% (95% CrI: 15.7%–18.9%) increase in cases/dog, while doubling at all three scales gave a 70.5% (95% CrI: 64.3%–76.8%) increase.

An increase in focal incidence was associated with decreased dog density and increased human:dog ratio in the focal village (Figs 3A, 4A). Random effects indicate that villages in the northeast of the district had higher than average incidence (Fig 3C).

We modelled the remaining three combinations of village/district and monthly/annual scales. Models at district level consistently failed to detect impacts of prior vaccination, even on removal of prior incidence (S2, S4 Tables, S9, S10, S12 Figs). Village-level annual models consistently detected effects of focal prior rolling coverage, but were inconsistent in detecting non-focal vaccination impacts (S3 Table, S11 Fig). Models at both village and district level without prior
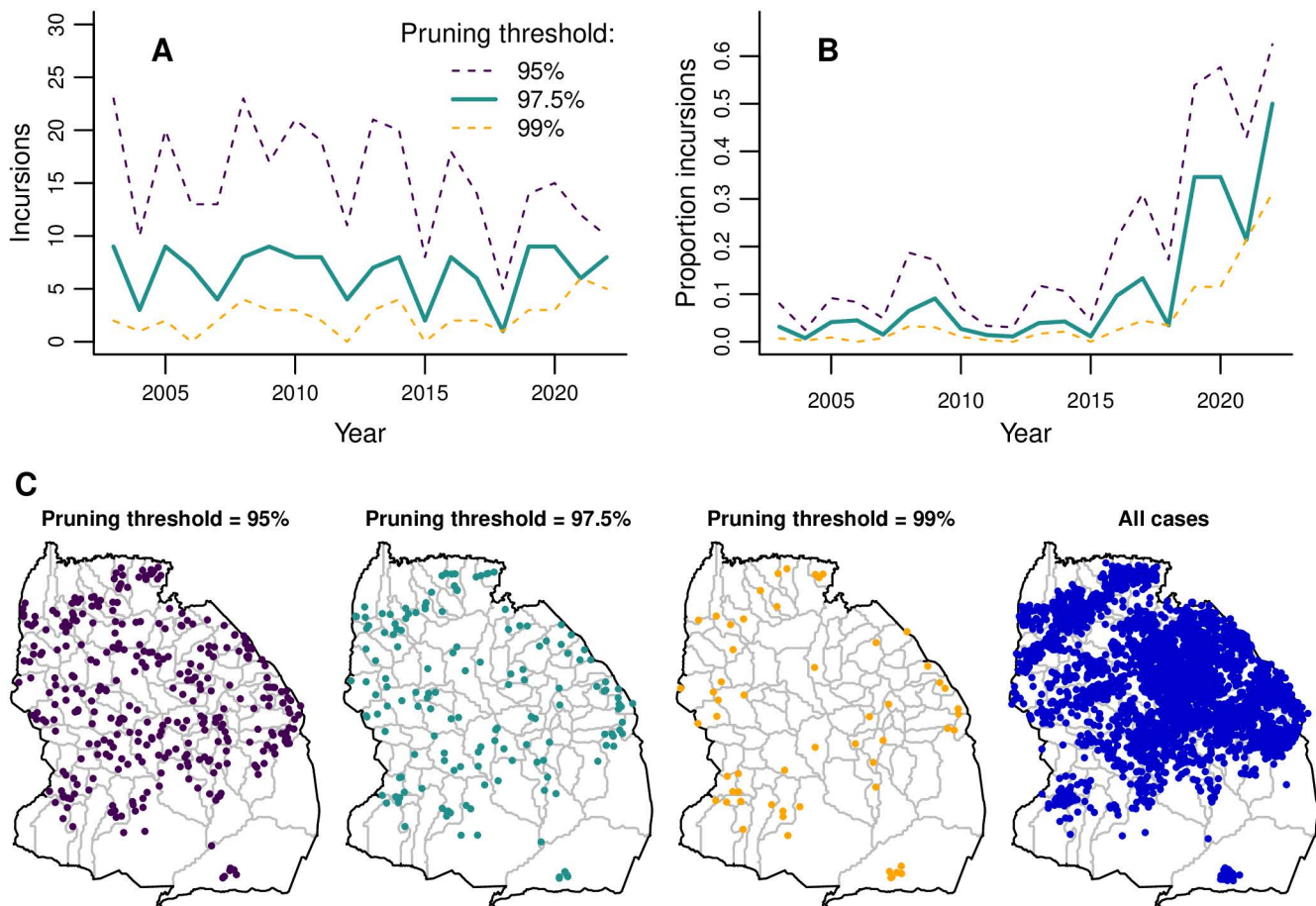
Fig 5. Estimated incursions in Serengeti District over time and space. (A) Annual numbers of incursions inferred from transmission trees with three different pruning thresholds. **(B)** Annual proportion of total rabies cases in carnivores that are inferred to be incursions. **(C)** Locations of inferred incursions under the three pruning thresholds. Locations of all carnivore cases are shown for comparison. Map of Serengeti villages developed by [41] and available at https://doi.org/10.5281/zenodo.6308051. The data underlying this figure can be found at https://doi.org/10.5281/zenodo.15012106.

https://doi.org/10.1371/journal.pbio.3002872.g005

incidence had a poorer fit to the data than the equivalent models with prior incidence (compare Fig 3D to S5D Fig and S7C Fig to S7D Fig).

A negative binomial distribution (mean = 0.39 (±0.013, standard error); size = 0.72 (±0.066)) fitted to the data on human exposures per rabid dog (S3 Fig) was used to simulate exposures from GLMM-based simulations of rabid dogs (Fig 3D). This provided a good match to observed exposures (Fig 3E).

By reconstructing transmission trees, we identified probable incursions into the district as cases without a plausible parent case within the 97.5th percentile of the distance kernel and serial interval distributions (S13 Fig, S5 Table). This 97.5% 'pruning threshold' prevents cases of unknown parentage (65.75% of all carnivore cases identified by contact tracing) being assigned a parent case that would lead to an improbably long serial interval or distance moved by a rabid animal (based on observations of known parent and offspring case pairs). Numbers of incursions remained relatively constant from 2003 to 2022 (Fig 5A, mean of 7 annual incursions). In contrast, the *proportion* of cases identified as incursions sharply increased (Fig 5B), from 3% pre-2018% to 26% post-2018, peaking at 50% in 2022. Incursion locations were more focused along the district's edges than cases in general (Fig 5C). Adjusting the pruning threshold to 95% or 99% impacted the number of inferred incursions, but led to qualitatively similar temporal and spatial patterns (Fig 5).

Discussion

We identify important drivers of rabies transmission from 20 years of fine-scale data on dog vaccination and from contact tracing. Under endemic rabies circulation, we find that outbreaks occur following multi-year periods when clusters of villages remain unvaccinated. However, when district-wide vaccination was made routine (spurred by the largest outbreak in 2010–2012) and spatial heterogeneity in coverage reduced, incidence declined to low levels (<0.4 cases per 1,000 dogs annually), attributable largely to short chains of transmission following incursions into the district. Prior rabies incidence focally (at the scale of the focal village) and across the district were the main drivers of current focal incidence, but were modulated by and correlated with prior focal vaccination coverage. When the masking effect of non-focal rabies incidence was removed, we also identified impacts of non-focal vaccination coverage and heterogeneity in this coverage. The role of prior incidence was highlighted in later years after vaccination had largely interrupted endemic transmission, when rabies did not re-surge despite late and incomplete vaccination campaigns. Reducing dog rabies cases had dramatic public health benefits, with corresponding reductions in human rabies exposures and deaths. However, frequent incursions inferred by transmission tree reconstruction suggest that benefits may be short-lived if dog vaccination lapses for extended periods.

Our analysis reveals how fine-scale variation in vaccination coverage drives rabies dynamics, with models aggregating coverage to district-level failing to show impacts on rabies incidence, demonstrating the limitations of coarsely aggregated data. Our empirical findings support simulation-based work arguing that gaps in coverage are detrimental for rabies control [36,38]. Pockets of low coverage are recognized as a driver of measles outbreaks in humans [47–50], but impacts of vaccination heterogeneity on incidence remain underexplored for other diseases, despite examples of vaccination heterogeneity existing in systems such as cholera [51] and COVID-19 [52]. The impact of this heterogeneity on disease incidence has rarely, if ever, been quantified in real systems, likely due to a lack of fine-scale data. Our work addresses this gap, providing evidence that the same level of vaccination coverage can have substantially different impacts, based on its spatial distribution. Future studies in human and animal disease systems may be aided by models that use spatial covariates to predict fine-scale vaccination coverage from coarser available data, e.g., sparse household surveys [53] or aggregated areal data [50]; though while these models may work well for routine childhood vaccinations, or potentially in animal contexts where vaccination is similarly routine, their transferability to the stochasticity arising from single-day village-level campaigns employed for dog rabies is unknown. The potential impact of clustered versus dispersed low-coverage villages also requires exploration. While we did not detect impacts of vaccination on incidence using coarse district-level data, striking 78.0%–85.5% declines in district-level incidence were associated with a 35% increase in prior district-level

coverage during large-scale rabies vaccination across 13 contiguous districts in south-east Tanzania, without accounting for heterogeneity [39]. These contrasting results were likely due to our focus on one district without wider-scale vaccination to reduce spread between districts. Our focus on a single, possibly idiosyncratic, time series may also be why the posterior for the parameter p that governs the heterogeneity effect lay outside the region that we *a priori* believed feasible; data from other areas could help refine estimates in future.

We find that vaccination controlled rabies despite not reaching the recommended 70% coverage target [25,37]. Some dog vaccination campaigns have faced similar difficulties in achieving high coverage [8,54], while others (even in Serengeti) have reported more success [25,55–57]. The low coverages we report may reflect our estimation methods [42]. We used vaccination records, with the dog population denominator derived from censuses and human:dog ratios. Methods like post-vaccination transects or household surveys may overestimate coverage if they rely on owner recall or do not cover unvaccinated sub-populations, resulting in bias towards more accessible areas and more visible (often adult) dogs [42,58]. Assuming constant human:dog ratios and a simple exponential human growth model in each village may have reduced the accuracy of our coverage estimates, while the relatively dense dog population and low human:dog ratio (estimated at 4.0 by the district human and dog census, relative to a country-wide estimate of 20.7 [59] and continent-wide estimate of 12.3 [60]) may have made campaigns challenging, contributing to true low coverage attainment. Nonetheless, district coverage only fell below 20% – the critical threshold estimated to push the reproductive number below one [45] – on <5% of months post-2007 (Fig 2C). So, while higher coverage would have achieved better (and faster) results, this relatively low vaccination threshold may be the reason why rabies was controlled to low levels of incidence regardless. Similarly, modelling suggests vaccination coverages of ≤40% could eliminate rabies [38] and protect against catastrophic declines in endangered canids [61]. We therefore conclude that, while high coverage should be the target for rapidly controlling disease, policymakers should not be deterred from introducing dog vaccination when achieving 70% coverage is challenging; if persistent spatial gaps are minimal, sub-optimal coverage still has major benefits due to rabies' low transmissibility [45] relative to human diseases that require higher levels of vaccination [62]. However, fast demographic rates still necessitate many dogs be vaccinated annually to maintain coverage, in comparison to childhood vaccination programs where higher coverage is reached through targeting a narrower demographic [63].

Impacts of prior rabies incidence at wider spatial scales on focal incidence indicate high epidemiological connectivity. These effects may be driven in part by vaccination at these spatial scales, either through reduced incidence in other vaccinated villages lowering the risk of rabid dogs roaming into the focal village or from dog owners in the focal village accessing vaccination campaigns in neighboring villages. Therefore, high coverage and resulting low incidence elsewhere mitigate local coverage gaps. In contrast, high coverage in a small area has only limited impact if the rest of the population is poorly vaccinated, consistent with the findings of previous simulation studies [38,64]. This interplay between dog vaccination and movement may have complex impacts on incidence that are also influenced by population configuration. Studies from Serengeti district [65] and Bali, Indonesia [66] found that impacts of prior incidence in other areas on focal rabies occurrence decreased with increasing distance from the focal village. We did not detect a reduced impact of non-bordering versus bordering villages on focal incidence, possibly because we studied only the collective impacts of villages at these scales (80+ non-bordering versus approximately 5 bordering); evaluating individual village impacts would be more likely to reveal distance-related effects. The observation that logging prior incidence (such that the rate of increase in focal incidence diminishes with increasing prior incidence) improves model fit is possibly a consequence of susceptible depletion, or local responses to outbreaks.

We anticipated that including prior incidence in our model would mask the effects of vaccination coverage at different spatial scales. This was confirmed in our results and was expected because prior incidence is partly driven by prior coverage. The strong effect of prior incidence, and the reduction in the quality of fit when prior incidence is removed from models, are also unsurprising. Prior incidence, in addition to incorporating part of the effect of prior vaccination, also incorporates information about actual transmission events that drive the force of infection coming both from within the district

and from incursions. Difficulties in separating out the impacts of correlated variables is a limitation of the GLMM framework. A mechanistic transmission model could more explicitly explore impacts of spatially heterogeneous vaccination, as per simulation studies [36,38,49]. However, this approach requires estimation of (or assumptions about) many parameters, and is vulnerable to assumptions about the important mechanisms to be included [67,68]. For these reasons, we explored GLMMs with and without the effect of prior incidence, to produce models both with a high quality of fit and from which we could extract independent effects of vaccination.

We inferred an average of 7 incursions annually, with incursions more frequent near district borders. Incursions in the district center likely result from human-mediated transport, which is an increasingly recognized problem [33,36,38,69,70]. Our inference methods have limitations; local transmission could be misidentified as incursions due to unobserved transmission, unusually long incubation periods or dog movements, while real incursions could go undetected within existing foci. We expect less misidentification at low incidence, suggesting inferred incursions should have increased post-2018. However, no increase was observed, possibly because real incursions decreased from the indirect effects of vaccination on circulation in neighboring districts and/or the direct impact of vaccination in those districts from 2020 [30,71]. Misidentification may contribute to fewer inferred incursions in the district center, where incidence was generally higher. Simulation studies could validate the performance of incursion assignment, and incorporating viral genomes may improve accuracy [33]. Regardless, the proportion of cases identified as incursions is far higher in later years (>20% of cases since 2019, reaching as high as 50% in 2022). This encouraging indication that local transmission has been interrupted, also serves as a warning that incursions are now a major driver of continued transmission and, no matter how well district-level control measures are implemented, elimination will require expanded vaccination. The example of Latin America shows how scaled up vaccination has largely eliminated dog-mediated rabies, with a contracting set of foci remaining in only the most challenging settings [22,40]. In Tanzania, rabies vaccination in Serengeti district began to extend across the surrounding Mara region in late 2020 [30,71]. Estimated incursions did not decline in 2021–2022, but this may change as rabies is controlled in neighboring districts.

A limitation of our rolling coverage estimates is the assumption that all dogs are equally likely to be vaccinated in each annual campaign. In reality, dog owners who chose not to attend a previous campaign may have had reasons (e.g., difficulty in handling dogs, distance to the vaccination point [58]) that make them likely to continue not to bring their dogs in subsequent years. Alternatively, attendees from previous campaigns may be less inclined to return, assuming their dogs are already protected. Given little data on these two behaviors, and evidence that repeat campaigns attract a mix of new and previously vaccinated dogs [25], we assumed the behaviors cancel out. However, this may have led to bias in our estimates. When calculating both campaign and rolling coverage, we also assume that the same dog is not vaccinated more than once a year. Campaigns were typically held for one day each year in each village, with rare follow-up vaccinations in response to outbreaks targeting unvaccinated dogs, and we expect owners are unlikely to bring their dogs to multiple campaigns in different villages in a year. However, owners could unknowingly revaccinate dogs that they recently acquired from another village, leading to overestimation of coverage.

A number of our results warrant further investigation. We consistently found a positive effect of human:dog ratio and negative effect of dog density on rabies incidence. We hypothesize that settings with higher human:dog ratios have less awareness of dog behavior, leading to rabies circulating with less intervention, while higher dog densities mean more cases are observed at the same incidence, leading to greater visibility and faster intervention. Studies of dog ownership practices in different settings and of how human responses to rabid dogs change based on recent incidence may increase understanding of these effects. We also observed that human rabies exposures from jackals and other wildlife were more common than by livestock, despite livestock comprising a higher proportion of animal cases than wildlife. There are multiple potential explanations for this; rabid livestock may be less aggressive and their bites easier to avoid, or wildlife cases that do not cause exposures less likely to be observed and thus under-represented in case data (compared to economically valued livestock).

Returning to our three initial hypotheses for why rabies continues to circulate despite control efforts, we conclude that: (1) spatial heterogeneity in dog vaccination was detrimental for control, and vaccination was only effective in interrupting endemic circulation when implemented consistently, underlining the importance of monitoring fine-scale coverage to promptly identify and address gaps; (2) mean coverage over the district was relatively low, but once heterogeneity was addressed, rabies was controlled nonetheless – a promising result given hard-to-reach populations with fast demographic rates; (3) Incursions from unvaccinated areas outside the district are frequent and now represent a major source of residual transmission. High epidemiological connectivity within the district, and frequent incursions from outside, interact with heterogeneous vaccination in complex ways that should be considered in program design. It is now vital that dog vaccination efforts be scaled up to ensure that impacts are sustained, to maximize their benefit to all, and to achieve the 'Zero by 30' goal.

Materials and methods

Ethical permissions

Ethical approval for this research was obtained from the Tanzania Commission for Science and Technology, the Institutional Review Boards of the National Institute for Medical Research in Tanzania and of Ifakara Health Institute, and the Ministry of Regional Administration and Local Government (NIMR/HQ/R.8a/vol.IX/300, NIMR/HQ/R.8a/vol.IX/994, NIMR/HQ/R.8a/vol.IX/2109, NIMR/HQ/ R.8a/vol.IX/2788, and IHI/IRB/No:22-2014).

Dog vaccination

We focus on the epidemiological dynamics of rabies in Serengeti District, northwest Tanzania from January 2002 to December 2022 using contact tracing and demographic data over the same period, and mass dog vaccination data with associated population estimates from January 2000 to December 2022 (to establish the level of pre-existing vaccination before the main study period). Between October 1996 and February 2001, four vaccination campaigns were carried out in Serengeti District [25]. These campaigns covered all the villages in the district as it was then, but we note that the district has since increased in area, with new villages incorporated that were previously part of the adjacent district, Musoma, and that were not covered in those earlier campaigns. Following the last of these four campaigns, a household survey estimated 73.7% coverage in the district. There was no vaccination in Serengeti district in 2002, but in 2003 Rabies Free Africa initiated annual campaigns in the villages in the East and South of the district, aiming to protect people and their animals and to prevent rabies spilling over into vulnerable carnivore populations in Serengeti National Park [43]. In 2004, vaccination campaigns were expanded to more villages with support from the District Veterinary Office.

Since then, dog vaccination typically takes place annually using a central point strategy where dogs are brought to a central location, such as a village center, church, or school in each village. A vehicle equipped with a loudspeaker is used to advertise vaccination the day before the campaign. Posters advertising the vaccination day are hung at busy locations within each village, such as village headquarters office, dispensaries, schools, churches and mosques. On vaccination days, dogs are registered, recording owner name, dog name, age, and sex. Rabies vaccination is offered free of charge using the Nobivac Rabies vaccine (MSD Animal Health, Boxmeer, the Netherlands). Dog owners receive a vaccination certificate for each vaccinated dog.

Since 2003, dogs have occasionally been vaccinated outside of central point campaigns in response to localized transmission. Since late 2020, villages in the northwest of the district have been part of a large-scale vaccination trial across Mara Region. A subset of those villages is following a continuous strategy, where vaccinations happen year-round [30] while the remaining villages continue annual central-point campaigns. Date, village and number of dogs vaccinated are available for all described vaccination events throughout the study and can be found in our GitHub repository: https://github.com/boydorr/Serengeti_vaccination_impacts.

Rabies incidence and exposures

Contact tracing was carried out following the methods outlined in Hampson and colleagues [45]. In brief, this involved collection of data on animal bite patients from health facilities, and rabid animal reports from livestock offices. Interviews with patients and owners of involved animals were conducted to gather details of these incidents and any connected possible cases or exposures, which were then also investigated. Animals were identified as probable cases on the basis of clinical signs and either: (1) disappearance or death within 10 days, or (2) being killed and either of unknown origin or known to have previously been bitten [45]. Probable rabies exposures were identified as any person receiving a bite/scratch from one of these probable animal cases. This approach generated data on 3,973 probable animal rabies cases – of which 3,362 were domestic dogs, 368 were livestock, 159 were wildlife, 81 were domestic cats, and three did not include a record of species – and 1,612 probable human rabies exposures in the years 2002–2022. It has previously been estimated that these methods identify 83%–95% of carnivore cases in the district [41]. Each probable animal case and probable human exposure was georeferenced and time-stamped, with the identity of the biting animal recorded where possible.

Dog population estimation

Human population counts were available at the village level from the 2012 government census [72], and at ward-level for the 2002 and 2022 censuses [73]. Village-level estimates for 2002 and 2022 were obtained by assuming that the population in each ward was divided between the villages in that ward in the same proportions as in 2012. For each village v, we then estimated the human population H for every month m in the period from January 2000 (i.e. $m = 1$) to December 2022 (i.e. $m = 276$) to be:

$$H_{v,m} = \alpha_v e^{r_v m}$$

(1)

Parameters a_v and r_v were estimated for each village by fitting Equation (1) to the three census populations (in 2002, 2012 and 2022) by non-linear least squares using the nls function from the stats package in R [74].

A georeferenced household census of humans and dogs in Serengeti District was completed between 2008 and 2016 [42], with each village censused once at some point during this period. This allowed estimation of village-specific human:dog ratios R_v. The dog population in every village each month was estimated as:

$$D_{v,m} = \frac{H_{v,m}}{R_v} \#$$

(2)

We also mapped the dog population to a grid of 1 km^2 cells by first assigning each cell to a village within Serengeti district. For each village, the dog population in each month ($D_{v,m}$) was then distributed among cells of that village in proportion to the number of dogs in those cells at the time of the georeferenced census.

Vaccination coverage

We calculated the numbers of dogs vaccinated in each village in each month in 2000–2022, $V_{v,m}$ To allow estimation of existing levels of vaccination at the time contact tracing began in 2002, we included information about the final vaccination campaign in the district prior to 2002, which was completed in 2000–2001 [25]. Monthly village-level data were not available for this campaign, so we assumed that the 73.7% of dogs estimated to have been vaccinated by post-vaccination household surveys (completed within two days of the vaccination campaign in each village) were distributed evenly across the campaign months (May 2000 to February 2001) in all villages that were part of the district at that time.

Village campaign coverages each year y (Fig 2E) were calculated as:

$$P_{v,y} = b\left(\sum_{\mu}\left(\frac{V_{v,\mu}}{D_{v,\mu}}\right)\right)\#$$

(3)

where μ are the months of y. This assumes that no dog is vaccinated twice within the same year. To prevent estimates of $P_{v,y} > 1$ (e.g., due to dog populations being underestimated or dogs being taken for vaccination outside their home village), we use a generalized sigmoidal bounding function $b(x)$:

$$b(x) = \frac{x}{(1+x^a)^{\frac{1}{a}}}\#$$

(4)

We selected $a = 6$ so that values of $x < 0.7$ (which represent 97% of village campaigns) experience little change, while $x = 1.0$ (an unrealistic achievement for campaigns in this setting) would be reduced to a more realistic 0.89 (S14 Fig). Annual district campaign coverages were calculated as:

$$P_y = 100\left(\sum_{\mu}\left(\frac{\sum_{v=1}^{88} V_{v,\mu}}{\sum_{v=1}^{88} D_{v,\mu}}\right)\right)\#$$

(5)

When estimating monthly village-level rolling vaccination coverages (i.e., the proportion of dogs in the population that have been vaccinated at least once since January 2000), we assume that numbers of vaccinated dogs decline geometrically each month with ratio:

$$\lambda = \sqrt[12]{1-d}\#$$

(6)

where $d = 0.448$ is the proportion of dogs that die in a year [75]. Assuming that all dogs are equally likely to be vaccinated each year, regardless of previous vaccination status, and that the same dog cannot be vaccinated twice in the same year, the number of vaccinated dogs in a village in a given month can be estimated as

$$N_{v,m} = b\left(\frac{(\lambda N_{v,m-1} + V_{v,m}(1-p_{v,m}))}{D_{v,m}}\right)D_{v,m}\#$$

(7)

where $p_{v,m}$ is the proportion of dogs that are available to be vaccinated this month (i.e., not already vaccinated in the current year) that had already been vaccinated in a previous year:

$$p_{v,m} = \frac{n_{v,m}}{D_{v,m}-(\lambda N_{v,m-1}-n_{v,m})}$$

(8)

and $n_{v,m}$ is the number of vaccinated dogs that were not vaccinated in the current year:

$$n_{v,m} = \begin{cases} \lambda N_{v,m-1} & \text{if January} \\ \lambda \max\left(0, n_{v,m-1} - V_{v,m-1}p_{v,m-1}\right) & \text{if any other month} \end{cases}$$

(9)

Finally, we obtained the rolling vaccination coverage for every village and month by:

$$C_{v,m} = \frac{N_{v,m}}{D_{v,m}}$$

(10)

and rolling vaccination coverage over the district in each month by:

$$C_m = \frac{\sum_{v=1}^{88} N_{v,m}}{\sum_{v=1}^{88} D_{v,m}}$$

(11)

The level of heterogeneity in rolling coverage over the district each month H_m was quantified using the population-weighted standard deviation in village rolling coverage:

$$H_m = \sqrt{\sum_{v=1}^{88} \left(d_{v,m} \left(C_{v,m} - \sum_{v=1}^{88} (d_{v,m} C_{v,m}) \right)^2 \right)}$$

(12)

where $d_{v,m}$ is the proportion of the district dog population living in village v in month m, i.e.:

$$d_{v,m} = \frac{D_{v,m}}{\sum_{v=1}^{88} D_{v,m}}$$

(13)

Modeling the impact of vaccination on rabies incidence

To investigate the impact of vaccination and other variables on rabies incidence, we developed a univariate negative binomial generalized linear mixed model (GLMM), where the single response variable was the number of probable dog rabies cases in a village in a given month. An offset equal to the log of the estimated dog population $D_{v,m}$ was included, allowing us to model incidence as cases per dog. Village was included as a random effect. Multiple fixed effects (each described in full below) were included together in the model including: (1) either rolling vaccination coverage or susceptibility (1 − rolling coverage) in the focal village over the prior two months; (2) either arithmetic mean coverage or power mean susceptibility over villages bordering the focal village over the prior two months; (3) either arithmetic mean coverage or power mean susceptibility over villages not bordering the focal village over the prior two months; (4) incidence in the focal village over the prior two months; (5) incidence over villages bordering the focal village over the prior two months; (6) incidence over villages not bordering the focal village over the prior two months; (7) dog density in the focal village in the current month; (8) the human:dog ratio in the focal village.

All analyses were conducted in R [74], with models fitted using Stan [76], via the RStan package [77] for models that included power means of susceptibility to allow estimation of both the power parameter p (Equation (14)) and the model coefficients and otherwise via the *brms* package [78]. For all variable coefficients we assumed a normal prior, $N(\mu = 0, \sigma = 100,000)$. For the size parameter of the negative binomial distribution, we use a gamma prior, $G(a = 0.01, \beta = 0.01)$ (the default prior selected for this parameter in *brms*). An exponential prior, $Exp(\lambda = 0.001)$, was used for the standard deviation of the village random effect. To discourage what we believed to be unrealistically large effects of heterogeneous coverage (S6 Fig), we used a normal prior for p centered on the arithmetic mean with a standard deviation of two, $N(\mu = 1, \sigma = 2)$. For models fitted in *brms*, we checked assumptions using simulated residuals via the DHARMa package [79].

Since >90% of rabies incubation periods recorded from contact tracing were less than two months, we include mean estimated vaccination coverage in the village v over the prior two months $(C_{v,m-1} + C_{v,m-2})/2$ as a fixed effect. As we also wanted to explore impacts of conditions in areas outside the focal village on focal incidence, we included fixed effects of mean vaccination coverage at two wider scales over the prior two months. The first of these was at the borders of the focal village. We obtained this variable by identifying all villages that shared a border with the focal village and calculating the proportion of the border shared with each of these villages using the *rgeos* package in R [80]. Bordering vaccination coverage in a given month was then calculated by multiplying these border proportions by vaccination coverages in these bordering villages, and summing over the bordering villages, i.e., the border-weighted arithmetic mean coverage. Vaccination coverage at borders with Serengeti National Park was assumed to be equal to the average of the vaccination coverages in the other bordering villages, and coverage at borders with the rest of Mara District was set to 9% (the coverage estimated in Serengeti District prior to mass vaccination campaigns [25]). Finally, we introduced a fixed effect of the prior population-weighted arithmetic mean

vaccination coverage over the dog populations of the rest of the district villages not sharing a border with the focal village.

To explore the impact of heterogeneity in coverage within the district on incidence in focal villages, we also considered a version of this model where the arithmetic mean coverages over bordering and non-bordering villages were replaced by power mean susceptibility (where susceptibility = 1 − coverage) at these scales. A power mean M_p over a sample, is calculated as:

$$M_p\left(x_1, \ldots, x_n\right) = \left(\frac{\sum_{i=1}^{n} w_i x_n^p}{\sum_{i=1}^{n} w_i}\right)^{\frac{1}{p}}$$

(14)

where w_i are the weights applied to each observation (length of shared border for mean susceptibility of bordering villages, and dog population for mean susceptibility of non-bordering villages). When fitting this model, we estimated the value of p in addition to the two GLMM coefficients for power mean susceptibility in bordering and non-bordering villages. We focus on power means of susceptibility rather than of vaccination coverage to enable calculation of logarithms of the power mean elements (to allow first-order approximation when p is close to zero and to provide stabilization at large p); vaccination coverages of zero are plausible and occur frequently in the data, while susceptibilities of zero are both implausible in this setting and corrected by Equation (4).

Current incidence of dog rabies was expected to be highly dependent on prior incidence, so we included an effect of mean incidence in the focal village over the prior two months. Prior incidence at the wider spatial scales was included as described for vaccination. Monthly incidence at borders with the rest of Mara Region was assumed to be 0.01/12, where 12 represents the number of months in the year and ∼0.01 was the highest proportion of Serengeti's dog population infected in any given year 1. This assumption is based on the rest of Mara Region being largely unvaccinated, and thus having generally high incidence. Incidence at the borders with Serengeti National Park was assumed to be equal to the average incidence in the other villages bordering a focal village. We compared a model where the prior incidence variables at each of the three spatial scales were logged with one where they were unlogged, selecting the best based on the lowest value of WAIC, a Bayesian model comparison statistic [46]. We also explored models where some of all of the prior incidence variables (which correlate with prior coverage/susceptibility) were removed (as outlined in Table 1), so as to estimate independent effects of coverage/susceptibility.

We incorporated fixed effects of the log of dog density in the village and the human:dog ratio R_v. When calculating dog density in a village we used the number of 1 km^2 grid cells assigned to the village that were occupied by at least one household during the Serengeti dog census as the denominator. This denominator was chosen to account for the fact that many villages, particularly on the North and South borders (Fig 1A), have large unoccupied areas that would otherwise bias density estimates.

In addition to the models described above, which use data at relatively fine spatiotemporal scales (village and month), we investigated the impact of aggregating data by fitting models at the remaining three combinations of village/district and monthly/annual scales. Prior distributions remained as previously specified. At the monthly, district scale, a univariate negative binomial generalized linear model (GLM) was fitted, where the single response variable was cases in the district each month, with an offset of the logged district dog population. Multiple fixed effect combinations were considered as outlined in S2 Table. These fixed effects included either rolling vaccination coverage at the district level (Equation (11)) or power mean susceptibility calculated over all 88 villages using Equation (14), both averaged over the prior two months. Monthly rabies incidence in the district was calculated by dividing the total cases that month by the estimated total district dog population that month, and again incorporated in the model as an average over the prior two months. District-level dog density was included by dividing the total district dog population each month by the number of occupied 1 km^2 grid cells in the district.

The third set of models at the annual, village scale, was fitted as univariate GLMMs with a response of the number of cases in a village in each year, with an offset of the logged mean village dog population that year. Prior vaccination at the three spatial scales (village, borders, rest of district) was incorporated in the form of the campaign coverage $P_{v,y}$ (Equation

(3)). We fitted models with fixed effects of: (1) $P_{v,y}$ last year; (2) Mean $P_{v,y}$ over the last two years; (3) Mean $P_{v,y}$ over the last three years; (4) $P_{v,y}$ last year and logged incidence last year. Log dog density and human:dog ratio in the focal village were also included in all four models, with village as a random effect. All fixed effect combinations are described in S3 Table.

Finally, we fitted a fourth set of models at the annual, district scale that were univariate GLMs with a response of cases in the district each year and an offset of the logged mean district dog population over that year. The campaign coverage in the district each year P_y (Equation (5)) was included in the same four combinations as for $P_{v,y}$ in the annual village-level models. All of these models included log dog density as a fixed effect (see S4 Table for details).

Annual models included fixed effects of campaign coverage rather than rolling coverage to make results comparable to a previous study of impacts of vaccination on rabies incidence [39]. The importance of dogs being carried over from previous campaigns was instead considered by our exploration of models that averaged prior campaign coverage over the previous 2–3 years.

Estimating incursions

To identify cases that likely originated from transmission outside Serengeti District (i.e., incursions), we reconstructed transmission trees using the *treerabid* package in R [41,81]. For this analysis, we excluded cases in herbivores, since these are unlikely to cause onward transmission, reducing the analyzed cases to 3,621. Tree reconstruction required distributions for the serial interval S (the time between onset of symptoms in an offspring case and in its parent case) and dispersal kernel K (the distance between cases and contacts regardless of whether these developed rabies). We calculated serial intervals from 1,156 paired dates of symptoms onset from cases and their recorded rabid biter and Euclidean distances between locations of 6,897 contacts and their recorded biter. For both S and K, we fitted gamma, lognormal and Weibull distributions using the fitdistrplus package [82], with the best-fitting distributions – lognormal for S and Weibull for K – chosen based on AIC (S5 Table). While fitting these distributions, censoring was applied for distances as described previously [41]. Distances of <100 m where the biter was a dog with known owner, and an accurate home location, were interval censored between 0 and 100 m to account for homestead sizes. For unknown dogs and wildlife, where locations were recorded for first observation rather than home location, the true distance to contacts was assumed unknown (right censored), but with a minimum of the recorded value or 100 m, whichever was larger, on the basis that biters from <100 m away would be recognized. Parameters of the fitted distributions (S5 Table) have changed little from those estimated previously [41], despite an additional seven years of contact tracing. A comparison of the data and best-fitting distributions is shown in S13 Fig.

The transmission tree reconstruction algorithm [81] was used to probabilistically assign a progenitor to each case i with no known rabid biter (65.75% of all carnivore cases). To be considered a possible progenitor of i, a case j has to have a symptoms onset date preceding that of i, and the serial interval and distance between i and j must be smaller than a selected quantile of the distributions S and K. This quantile, known as the pruning threshold, is chosen to prevent assignment of progenitors that are unlikely to be correct given the separation of cases in space or time. We explored pruning thresholds of 0.95, 0.975, and 0.99; the maximum serial intervals and distances defined by these thresholds are given in S5 Table. The probability of each case $j \in \{1,...,n\}$ that meets these pruning criteria being randomly selected as the progenitor of i is:

$$p_{ij} = \frac{S_{ij}K_{ij}}{\sum_{k=1}^{n} S_{ik}K_{ik}}$$

(15)

where S_{ij} and K_{ij} are the probabilities of the serial interval and distance between i and j based on reference distributions S and K. In cases where $n = 0$, no biter was assigned, with i being assumed to be an incursion. To account for recorded uncertainties in the timing of bites and symptoms onset, 1,000 bootstrapped datasets were generated by drawing dates

randomly from a uniform distribution over the recorded uncertainty window, while preserving the correct sequence of events between known parent and offspring cases. We used the best-fitting lognormal distribution for S (S5 Table) and when i was a dog with known owner and accurate location we used the best-fitting Weibull distribution for K. When i was an unknown dog or wildlife, where the recorded location was generally the location i was observed biting, not i's home location, K was a Weibull distribution fitted to simulations of the Euclidean distance travelled as a result of two draws from the previously fitted Weibull with a uniform random change in direction between them (representing the movement of j to i, followed by the movement of i to its recorded location). For each pruning threshold, we identified probable incursions as those cases identified as an incursion more frequently than they were assigned to any other progenitor within the set of 1,000 bootstrapped trees. Inferred incursions and proportion incursions were notably high in 2002, as an expected artefact of beginning contact tracing, and are thus not considered in the results. Progenitors of some 2002 cases likely occurred in 2001, and thus would have gone undetected. Additionally, detection was likely lower in 2002 as methods were still being honed.

Supporting information

S1 Video. Monthly spatial distribution of dog cases, human exposures and dog vaccination coverage over the study period. Estimated vaccination coverage at the village-level for each month in 2002–2022 is indicated by the color scale. Locations of dog cases (blue points), human exposures (purple triangles) and human. Map of Serengeti villages developed by [41] and available at https://doi.org/10.5281/zenodo.6308051. The data underlying this Video can be found at https://doi.org/10.5281/zenodo.15012106.
(MP4)

S1 Fig. Campaign vaccination coverage each year from 2002 to 2022 A) at district level and B) at village level. Map of Serengeti villages developed by [41] and available at https://doi.org/10.5281/zenodo.6308051. The data underlying this figure can be found at https://doi.org/10.5281/zenodo.15012106.
(PDF)

S2 Fig. Mean of and spatial heterogeneity in rolling vaccination coverage each year. (A) The mean rolling vaccination coverage in Serengeti District over each year (12-month averages of the values in Fig 2C) is indicated by the solid black line. Mean rolling coverages each year for 8 randomly selected villages is indicated by dashed colored lines. **(B)** The weighted standard deviation in the rolling vaccination coverage over the villages in Serengeti District (yearly means of the values in Fig 2C). **(C)** Mean rolling vaccination coverage in each village over each year from 2002 to 2022 is indicated by the color scale. Map of Serengeti villages developed by [41] and available at https://doi.org/10.5281/zenodo.6308051. The data underlying this figure can be found at https://doi.org/10.5281/zenodo.15012106.
(PDF)

S3 Fig. Human exposures per rabid dog. Histogram of human rabies exposures by each rabid dog from contact tracing data (grey bars), with fitted negative binomial distribution (blue line). The data underlying this figure can be found at https://doi.org/10.5281/zenodo.15012106.
(PDF)

S4 Fig. Probable human exposures by dogs versus by all other species from contact tracing. The data underlying this figure can be found at https://doi.org/10.5281/zenodo.15012106.
(PDF)

S5 Fig. Impact of removing prior cases/dog explanatory variables from the monthly village-level GLMM for current cases per dog (compare with Fig 3). (A) Exponentiated standardized values of the coefficients estimated for each

explanatory variable, with 95% CrIs. **(B)** Line shows the expected cases/1,000 dogs (number of dog cases normalized by dog population) in a village this month for different mean rolling vaccination coverages across the focal village and district in the prior 2 months. Shaded areas show 95% credible intervals (CrIs), and predictions were obtained using average values of unspecified explanatory variables. **(C)** Exponentiated random effect values for each village in the district. **(D)** Comparison of observed monthly dog cases (points) with the 95% prediction interval from the fitted model. Data points in red fall outside the 95% prediction interval (PI). Map of Serengeti villages developed by [41] and available at https://doi. org/10.5281/zenodo.6308051. The data underlying this figure can be found at https://doi.org/10.5281/zenodo.15012106. (PDF)

S6 Fig. The impact of different powers on the power mean of susceptibility under different levels of heterogeneous vaccination. Here we assume a landscape where an increasing proportion of the area is vaccinated to 70% (30% susceptibility) while the remaining proportion remains at 0% coverage (100% susceptibility). We then calculate **(A)** the power mean susceptibility and **(B)** the effective coverage (1 – power mean susceptibility) at each proportion of area vaccinated at a range of values of the power p (Equation (14)). $p = 1$ is the arithmetic mean, and represents a scenario where, for a given proportion of dogs being vaccinated, the effective level of vaccination is the same regardless of how these vaccinated dogs are distributed over the area, i.e., heterogeneity in vaccination does not reduce (or increase) the impact of that vaccination on rabies cases. We used these curves showing the impact of different powers to select the prior distribution for $p \sim N(\mu = 1, \sigma = 2)$. If 99% of the area is covered, then the arithmetic mean coverage is 69.3%. If $p = 2$, then the effective coverage for the heterogeneous landscape is 68.5%; 0.8% lower than if vaccination had been homogeneous. If $p = 5$, however, effective coverage would be 58.4%, which is 10.9% below the arithmetic mean, despite only 1% of the area being uncovered, which seems an excessively large effect. The choice of $\sigma = 2$ was therefore made to exclude $p \geq 5$ from the a priori confidence interval. The data underlying this figure can be found at https://doi.org/10.5281/zenodo.15012106. (PDF)

S7 Fig. Impact of power mean susceptibility on rabies incidence at the village level and quality of model fits to data. (A–B) Expected cases/1,000 dogs in a village from models with **(A)** and without **(B)** effects of prior incidence beyond the village. Predictions are shown for different mean susceptibilities (assuming homogeneous vaccination, i.e., power mean susceptibilities beyond the village equal susceptibility in the village) and mean cases/dog in the prior 2 months. Prior cases/dog values represent the observed district-level range and shaded areas show 95% CrIs, Predictions were obtained using average values of unspecified explanatory variables. **(C–D)** Comparison of observed monthly dog cases (points) with the 95% prediction interval from the fitted model with **(C)** or without **(D)** prior incidence beyond the village. Data points in red fall outside the 95% prediction interval (PI). The data underlying this figure can be found at https://doi.org/10.5281/zenodo.15012106. (PDF)

S8 Fig. Difference between power mean and arithmetic mean susceptibility. Difference between power mean susceptibility calculated over all villages in the district using fitted values of p from the model without prior incidence beyond the focal village (Fig 4C) minus the arithmetic mean for each month **(A)** or averaged over each year **(B)**. The data underlying this figure can be found at https://doi.org/10.5281/zenodo.15012106. (PDF)

S9 Fig. Modelling monthly dog rabies cases in Serengeti District at district level. (A) Expected cases/dog (number of dog cases normalized by dog population) in the district this month for different mean rolling vaccination coverages and mean cases/dog in the prior 2 months. Shaded areas show 95% CrIs, points show the data, and predictions were obtained using the average value of dog density. **(B)** Exponentiated standardized values of the coefficients estimated for

each explanatory variable, with 95% CrIs. Coefficients obtained for a version of the model fitted without prior cases/dog as an explanatory variable are included for comparison. See S2 Table for tabulated parameter values. **(C)** Comparison of observed monthly dog cases (points) with the 95% prediction interval from the fitted model. Data points in red fall outside the 95% prediction interval (PI). The data underlying this figure can be found at https://doi.org/10.5281/zenodo.15012106. (PDF)

S10 Fig. Using power mean susceptibility to model impacts of heterogeneity in rolling vaccination on district-level incidence. (A) Exponentiated standardized estimated coefficients for each explanatory variable, with 95% CrIs. **(B)** Estimated power p used to calculate power mean susceptibility. In **A–B**, estimates from models with and without effects of prior incidence are shown. See S2 Table for tabulated parameter values. The data underlying this figure can be found at https://doi.org/10.5281/zenodo.15012106. (PDF)

S11 Fig. Annual village-level GLMM for current cases per dog. Lines show the expected cases per 1,000 dogs (number of dog cases normalized by dog population) in a village this year for different campaign vaccination coverages and cases per 1,000 dogs in the previous year. Prior incidence values were chosen to represent the range observed at district level. Shaded areas show 95% CrIs, and predictions were obtained using average values of unspecified explanatory variables. See S3 Table for tabulated parameter values. The data underlying this figure can be found at https://doi.org/10.5281/zenodo.15012106. (PDF)

S12 Fig. Annual district-level GLM for cases per dog. Lines show the expected cases per 1,000 dogs (number of dog cases normalized by dog population) in the district this year for different campaign vaccination coverages and cases per 1,000 dogs in the previous year. Prior incidence values were chosen to represent the range observed at district level. Shaded areas show 95% CrIs, and predictions were obtained using average values of unspecified explanatory variables. See S4 Table for tabulated parameter values. The data underlying this figure can be found at https://doi.org/10.5281/zenodo.15012106. (PDF)

S13 Fig. Serial interval distribution and distance kernel. (A) Histogram of serial intervals calculated from contact tracing data (grey bars), with fitted lognormal distribution (blue line). **(B)** Histogram of distances between the starting location of a case and the locations of its contacts (grey bars), with fitted Weibull distribution (blue line). The data underlying this figure can be found at https://doi.org/10.5281/zenodo.15012106. (PDF)

S14 Fig. Bounding the proportion of dogs vaccinated between zero and one. Illustration of the function $b(x) = x/((1+x^a)^{1/a})$ used to bound coverage estimates below one. Throughout our analyses, we set $a = 6$ when applying this function, but the impact of using alternative values is shown here. The data underlying this figure can be found at https://doi.org/10.5281/zenodo.15012106. (PDF)

S1 Table. Vaccination of Serengeti District by year. Numbers of dogs that received a vaccination in each year, campaign coverage (percentage of the district dog population vaccinated in campaigns each year), and campaign completeness (percentage of villages in the district that held a campaign in each year). (DOCX)

S2 Table. Parameter estimates for monthly district-level GLMs for cases/dog in the district in the current month. Ninety-five percent credible intervals (CrIs) in brackets. Coefficients for fixed effects where the 95% CrI does not include

zero are marked *. Predictions from model 1 (and coefficients for model 2) are presented in S9 Fig). Parameters from models 3 and 4 are illustrated in S10 Fig. Vaccination, susceptibility and cases/dog variables are all averages over the prior two months.
(DOCX)

S3 Table. Coefficients for the annual village-level negative binomial GLMMs. Ninety-five percent credible intervals in brackets. Coefficients for fixed effects where the 95% CrI does not include zero are marked *. Predictions from the model 4 (including campaign coverage and cases/dog in the last year as explanatory variables) are presented in S11 Fig.
(DOCX)

S4 Table. Coefficients for the annual district-level negative binomial GLMs. Ninety-five percent credible intervals in brackets. Coefficients for fixed effects where the 95% CrI does not include zero are marked *. Predictions from model 4 (including campaign coverage and cases/dog in the last year as explanatory variables) are presented in S12 Fig.
(DOCX)

S5 Table. Fitted distributions for incubation period (units = days), serial interval (units = days) and distance kernel (units = meters). For each epidemiological variable calculated from the contact tracing data with sample size *n*, we fitted gamma, lognormal and Weibull distributions. Estimates of the parameters for each distribution are provided. The best fitting model for each epidemiological variable based on AIC is highlighted in bold. The 95th, 97.5th and 99th percentiles of each distribution are given.
(DOCX)

Acknowledgments

Author contributions

Conceptualization: Elaine Ferguson, Katie Hampson.

Data curation: Elaine Ferguson, Danni Anderson.

Formal analysis: Elaine Ferguson, Jonathan Dushoff.

Funding acquisition: Katie Hampson, Felix Lankester.

Investigation: Ahmed Lugelo, Anna Czupryna, Lwitiko Sikana.

Methodology: Elaine Ferguson, Jonathan Dushoff, Katie Hampson.

Project administration: Felix Lankester, Katie Hampson.

Software: Elaine Ferguson.

Supervision: Jonathan Dushoff, Katie Hampson.

Validation: Elaine Ferguson.

Visualization: Elaine Ferguson.

Writing – original draft: Elaine Ferguson, Anna Czupryna, Katie Hampson.

Writing – review & editing: Elaine Ferguson, Anna Czupryna, Felix Lankester, Jonathan Dushoff, Katie Hampson.

References

1. Lavan RP, King AIM, Sutton DJ, Tunceli K. Rationale and support for a One Health program for canine vaccination as the most cost-effective means of controlling zoonotic rabies in endemic settings. Vaccine. 2017;35(13):1668–74. https://doi.org/10.1016/j.vaccine.2017.02.014 PMID: 28216188.

2. Tidman R, Thumbi SM, Wallace R, de Balogh K, Iwar V, Dieuzy-Labaye I, et al. United against rabies forum: the one health concept at work. Front Public Health. 2022;10:854419. https://doi.org/10.3389/fpubh.2022.854419 PMID: 35493394.

3. Schreiner CL, Nuismer SL, Basinski AJ. When to vaccinate a fluctuating wildlife population: Is timing everything? J Appl Ecol. 2020;57(2):307–19. https://doi.org/10.1111/1365-2664.13539 PMID: 32139945.

4. Lesnoff M, Peyre M, Duarte PC, Renard J-F, Mariner JC. A simple model for simulating immunity rate dynamics in a tropical free-range poultry population after avian influenza vaccination. Epidemiol Infect. 2009;137(10):1405–13. https://doi.org/10.1017/S0950268809002453 PMID: 19327199.

5. Peel AJ, Pulliam JRC, Luis AD, Plowright RK, O'Shea TJ, Hayman DTS, et al. The effect of seasonal birth pulses on pathogen persistence in wild mammal populations. Proc Biol Sci. 2014;281(1786):20132962. https://doi.org/10.1098/rspb.2013.2962 PMID: 24827436.

6. Altizer S, Bartel R, Han BA. Animal migration and infectious disease risk. Science. 2011;331(6015):296–302. https://doi.org/10.1126/science.1194694 PMID: 21252339.

7. Tatem AJ, Rogers DJ, Hay SI. Global transport networks and infectious disease spread. Adv Parasitol. 2006;62:293–343. https://doi.org/10.1016/S0065-308X(05)62009-X PMID: 16647974.

8. Muthiani Y, Traoré A, Mauti S, Zinsstag J, Hattendorf J. Low coverage of central point vaccination against dog rabies in Bamako, Mali. Prev Vet Med. 2015;120(2):203–9. https://doi.org/10.1016/j.prevetmed.2015.04.007 PMID: 25953653.

9. Lim PC, Lembo T, Hampson K, Changalucha J, Sambo M, Ghosal S. Tackling barriers to collective action for effective vaccination campaigns: rabies in rural Africa as an example. Humanit Soc Sci Commun. 2022;9(1):364. https://doi.org/10.1057/s41599-022-01374-3 PMID: 38726049.

10. Duamor CT, Hampson K, Lankester F, Lugelo A, Mpolya E, Kreppel K, et al. Development, feasibility and potential effectiveness of community-based continuous mass dog vaccination delivery strategies: lessons for optimization and replication. PLoS Negl Trop Dis. 2022;16(9):e0010318. https://doi.org/10.1371/journal.pntd.0010318 PMID: 36067231.

11. Woodroffe R. Assessing the risks of intervention: immobilization, radio-collaring and vaccination of African wild dogs. Oryx. 2001;35(3):234–44. https://doi.org/10.1046/j.1365-3008.2001.00186.x

12. Hampson K, Coudeville L, Lembo T, Sambo M, Kieffer A, Attlan M, et al. Estimating the global burden of endemic canine rabies. PLoS Negl Trop Dis. 2015;9(4):e0003709. https://doi.org/10.1371/journal.pntd.0003709 PMID: 25881058.

13. World Health Organization. WHO Expert Consultation on Rabies: second report. Geneva: World Health Organization; 2013. Available: https://iris.who.int/handle/10665/85346

14. Hampson K, Dobson A, Kaare M, Dushoff J, Magoto M, Sindoya E, et al. Rabies exposures, post-exposure prophylaxis and deaths in a region of endemic canine rabies. PLoS Negl Trop Dis. 2008;2(11):e339. https://doi.org/10.1371/journal.pntd.0000339 PMID: 19030223.

15. Sambo M, Cleaveland S, Ferguson H, Lembo T, Simon C, Urassa H, et al. The burden of rabies in Tanzania and its impact on local communities. PLoS Negl Trop Dis. 2013;7(11):e2510. https://doi.org/10.1371/journal.pntd.0002510 PMID: 24244767.

16. Changalucha J, Steenson R, Grieve E, Cleaveland S, Lembo T, Lushasi K, et al. The need to improve access to rabies post-exposure vaccines: lessons from Tanzania. Vaccine. 2019;37 Suppl 1(Suppl 1):A45–53. https://doi.org/10.1016/j.vaccine.2018.08.086 PMID: 30309746.

17. Wera E, Mourits MCM, Hogeveen H. Cost-effectiveness of mass dog rabies vaccination strategies to reduce human health burden in Flores Island, Indonesia. Vaccine. 2017;35(48):6727–36. https://doi.org/10.1016/j.vaccine.2017.10.009

18. Fitzpatrick MC, Hampson K, Cleaveland S, Mzimbiri I, Lankester F, Lembo T, et al. Cost-effectiveness of canine vaccination to prevent human rabies in rural Tanzania. Ann Intern Med. 2014;160(2):91–100. https://doi.org/10.7326/M13-0542 PMID: 24592494.

19. Zinsstag J, Dürr S, Penny MA, Mindekem R, Roth F, Menendez Gonzalez S, et al. Transmission dynamics and economics of rabies control in dogs and humans in an African city. Proc Natl Acad Sci U S A. 2009;106(35):14996–5001. https://doi.org/10.1073/pnas.0904740106 PMID: 19706492.

20. World Health Organisation. Zero by 30: the global strategic plan to end human deaths from dog-mediated rabies by 2030. 2018. Available: https://www.who.int/publications/i/item/9789241513838.

21. Kamata Y, Tojinbara K, Hampson K, Makita K. The final stages of dog rabies elimination from Japan. Zoonoses Public Health. 2023;70(1):1–12. https://doi.org/10.1111/zph.12989 PMID: 35931921.

22. Vigilato MAN, Clavijo A, Knobl T, Silva HMT, Cosivi O, Schneider MC, et al. Progress towards eliminating canine rabies: policies and perspectives from Latin America and the Caribbean. Philos Trans R Soc Lond B Biol Sci. 2013;368(1623):20120143. https://doi.org/10.1098/rstb.2012.0143 PMID: 23798691.

23. World Health Organisation. Mexico is free from human rabies transmitted by dogs. 2019 [cited 7 Feb 2024]. Available: https://www.who.int/news/item/21-12-2019-mexico-is-free-from-human-rabies-transmitted-by-dogs.

24. Gibson AD, Yale G, Corfmat J, Appupillai M, Gigante CM, Lopes M, et al. Elimination of human rabies in Goa, India through an integrated One Health approach. Nat Commun. 2022;13(1):2788. https://doi.org/10.1038/s41467-022-30371-y PMID: 35589709.

25. Cleaveland S, Kaare M, Tiringa P, Mlengeya T, Barrat J. A dog rabies vaccination campaign in rural Africa: impact on the incidence of dog rabies and human dog-bite injuries. Vaccine. 2003;21(17–18):1965–73. https://doi.org/10.1016/s0264-410x(02)00778-8 PMID: 12706685.

26. Zinsstag J, Lechenne M, Laager M, Mindekem R, Naïssengar S, Oussiguéré A, et al. Vaccination of dogs in an African city interrupts rabies transmission and reduces human exposure. Sci Transl Med. 2017;9(421):eaaf6984. https://doi.org/10.1126/scitranslmed.aaf6984 PMID: 29263230.

27. Lapiz SMD, Miranda MEG, Garcia RG, Daguro LI, Paman MD, Madrinan FP, et al. Implementation of an intersectoral program to eliminate human and canine rabies: the Bohol Rabies Prevention and Elimination Project. PLoS Negl Trop Dis. 2012;6(12):e1891. https://doi.org/10.1371/journal.pntd.0001891 PMID: 23236525.

28. Lembo T, Hampson K, Kaare MT, Ernest E, Knobel D, Kazwala RR, et al. The feasibility of canine rabies elimination in Africa: dispelling doubts with data. PLoS Negl Trop Dis. 2010;4(2):e626. https://doi.org/10.1371/journal.pntd.0000626 PMID: 20186330.

29. Sambo M, Ferguson EA, Abela-Ridder B, Changalucha J, Cleaveland S, Lushasi K, et al. Scaling-up the delivery of dog vaccination campaigns against rabies in Tanzania. PLoS Negl Trop Dis. 2022;16(2):e0010124. https://doi.org/10.1371/journal.pntd.0010124 PMID: 35143490.

30. Lugelo A, Hampson K, Ferguson EA, Czupryna A, Bigambo M, Duamor CT, et al. Development of dog vaccination strategies to maintain herd immunity against rabies. Viruses. 2022;14(4):830. https://doi.org/10.3390/v14040830 PMID: 35458560.

31. Davlin S, Lapiz SM, Miranda ME, Murray K. Factors associated with dog rabies vaccination in Bhol, Philippines: results of a cross-sectional cluster survey conducted following the island-wide rabies elimination campaign. Zoonoses Public Hlth. 2013;60(7):494–503. https://doi.org/10.1111/zph.12026 PMID: 23280122.

32. Lankester F, Hampson K, Lembo T, Palmer G, Taylor L, Cleaveland S. Infectious disease. Implementing Pasteur's vision for rabies elimination. Science. 2014;345(6204):1562–4. https://doi.org/10.1126/science.1256306 PMID: 25258065.

33. Lushasi K, Brunker K, Rajeev M, Ferguson EA, Jaswant G, Baker LL, et al. Integrating contact tracing and whole-genome sequencing to track the elimination of dog-mediated rabies: an observational and genomic study. Elife. 2023;12:e85262. https://doi.org/10.7554/eLife.85262 PMID: 37227428.

34. Tohma K, Saito M, Demetria CS, Manalo DL, Quiambao BP, Kamigaki T, et al. Molecular and mathematical modeling analyses of inter-island transmission of rabies into a previously rabies-free island in the Philippines. Infect Genet Evol. 2016;38:22–8. https://doi.org/10.1016/j.meegid.2015.12.001 PMID: 26656835.

35. Castillo-Neyra R, Toledo AM, Arevalo-Nieto C, MacDonald H, De la Puente-León M, Naquira-Velarde C, et al. Socio-spatial heterogeneity in participation in mass dog rabies vaccination campaigns, Arequipa, Peru. PLoS Negl Trop Dis. 2019;13(8):e0007600. https://doi.org/10.1371/journal.pntd.0007600 PMID: 31369560.

36. Ferguson EA, Hampson K, Cleaveland S, Consunji R, Deray R, Friar J, et al. Heterogeneity in the spread and control of infectious disease: consequences for the elimination of canine rabies. Sci Rep. 2015;5:18232. https://doi.org/10.1038/srep18232 PMID: 26667267.

37. Coleman PG, Dye C. Immunization coverage required to prevent outbreaks of dog rabies. Vaccine. 1996;14(3):185–6. https://doi.org/10.1016/0264-410x(95)00197-9 PMID: 8920697.

38. Townsend SE, Sumantra IP, , Bagus GN, Brum E, Cleaveland S, et al. Designing programs for eliminating canine rabies from islands: Bali, Indonesia as a case study. PLoS Negl Trop Dis. 2013;7(8):e2372. https://doi.org/10.1371/journal.pntd.0002372 PMID: 23991233.

39. Hayes S, Lushasi K, Sambo M, Changalucha J, Ferguson EA, Sikana L, et al. Understanding the incidence and timing of rabies cases in domestic animals and wildlife in south-east Tanzania in the presence of widespread domestic dog vaccination campaigns. Vet Res. 2022;53(1):106. https://doi.org/10.1186/s13567-022-01121-1 PMID: 36510331.

40. Rysava K, Mancero T, Caldas E, de Carvalho MF, Castro APB, Gutiérrez V, et al. Towards the elimination of dog-mediated rabies: development and application of an evidence-based management tool. BMC Infect Dis. 2020;20(1):778. https://doi.org/10.1186/s12879-020-05457-x PMID: 33081712.

41. Mancy R, Rajeev M, Lugelo A, Brunker K, Cleaveland S, Ferguson EA, et al. Rabies shows how scale of transmission can enable acute infections to persist at low prevalence. Science. 2022;376(6592):512–6. https://doi.org/10.1126/science.abn0713 PMID: 35482879.

42. Sambo M, Johnson PCD, Hotopp K, Changalucha J, Cleaveland S, Kazwala R, et al. Comparing methods of assessing dog rabies vaccination coverage in rural and urban communities in Tanzania. Front Vet Sci. 2017;4:33. https://doi.org/10.3389/fvets.2017.00033 PMID: 28352630.

43. Cleaveland S, Mlengeya T, Kaare M, Haydon D, Lembo T, Laurenson MK, et al. The conservation relevance of epidemiological research into carnivore viral diseases in the Serengeti. Conserv Biol. 2007;21(3):612–22. https://doi.org/10.1111/j.1523-1739.2007.00701.x PMID: 17531040.

44. Viana M, Cleaveland S, Matthiopoulos J, Halliday J, Packer C, Craft ME, et al. Dynamics of a morbillivirus at the domestic-wildlife interface: Canine distemper virus in domestic dogs and lions. Proc Natl Acad Sci U S A. 2015;112(5):1464–9. https://doi.org/10.1073/pnas.1411623112 PMID: 25605919.

45. Hampson K, Dushoff J, Cleaveland S, Haydon DT, Kaare M, Packer C, et al. Transmission dynamics and prospects for the elimination of canine rabies. PLoS Biol. 2009;7(3):e53. https://doi.org/10.1371/journal.pbio.1000053 PMID: 19278295.

46. Watanabe S. Asymptotic equivalence of Bayes cross validation and widely applicable information criterion in singular learning theory. J Mach Learn Res. 2010;11:3571–94.

47. van den Hof S, Meffre CM, Conyn-van Spaendonck MA, Woonink F, de Melker HE, van Binnendijk RS. Measles outbreak in a community with very low vaccine coverage, the Netherlands. Emerg Infect Dis. 2001;7(3 Suppl):593–7. https://doi.org/10.3201/eid0707.010743 PMID: 11485681.

48. Truelove SA, Graham M, Moss WJ, Metcalf CJE, Ferrari MJ, Lessler J. Characterizing the impact of spatial clustering of susceptibility for measles elimination. Vaccine. 2019;37(5):732–41. https://doi.org/10.1016/j.vaccine.2018.12.012 PMID: 30579756.

49. Masters NB, Eisenberg MC, Delamater PL, Kay M, Boulton ML, Zelner J. Fine-scale spatial clustering of measles nonvaccination that increases outbreak potential is obscured by aggregated reporting data. Proc Natl Acad Sci U S A. 2020;117(45):28506–14. https://doi.org/10.1073/pnas.2011529117 PMID: 33106403.

50. Utazi CE, Thorley J, Alegana VA, Ferrari MJ, Nilsen K, Takahashi S, et al. A spatial regression model for the disaggregation of areal unit based data to high-resolution grids with application to vaccination coverage mapping. Stat Methods Med Res. 2019;28(10–11):3226–41. https://doi.org/10.1177/0962280218797362 PMID: 30229698.

51. Ali M, Emch M, Yunus M, Clemens J. Modeling spatial heterogeneity of disease risk and evaluation of the impact of vaccination. Vaccine. 2009;27(28):3724–9. https://doi.org/10.1016/j.vaccine.2009.03.085 PMID: 19464555.

52. Tiu A, Susswein Z, Merritt A, Bansal S. Characterizing the spatiotemporal heterogeneity of the Covid-19 vaccination landscape. Am J Epidemiol. 2022;191(10):1792–802. https://doi.org/10.1093/aje/kwac080 PMID: 35475891.

53. Utazi CE, Thorley J, Alegana VA, Ferrari MJ, Takahashi S, Metcalf CJE, et al. High resolution age-structured mapping of childhood vaccination coverage in low and middle income countries. Vaccine. 2018;36(12):1583–91. https://doi.org/10.1016/j.vaccine.2018.02.020 PMID: 29454519.

54. Ferguson AW, Muloi D, Ngatia DK, Kiongo W, Kimuyu DM, Webala PW, et al. Volunteer based approach to dog vaccination campaigns to eliminate human rabies: lessons from Laikipia County, Kenya. PLoS Negl Trop Dis. 2020;14(7):e0008260. https://doi.org/10.1371/journal.pntd.0008260 PMID: 32614827.

55. Perry BD, Kyendo TM, Mbugua SW, Price IE, Varma S. Increasing rabies vaccination coverage in urban dog populations of high human population density suburbs: a case study in Nairobi, Kenya. Prev Vet Med. 1995;22(1–2):137–42. https://doi.org/10.1016/0167-5877(94)00407-a

56. Léchenne M, Oussiguere A, Naissengar K, Mindekem R, Mosimann L, Rives G, et al. Operational performance and analysis of two rabies vaccination campaigns in N'Djamena, Chad. Vaccine. 2016;34(4):571–7. https://doi.org/10.1016/j.vaccine.2015.11.033 PMID: 26631415.

57. Sánchez-Soriano C, Gibson AD, Gamble L, Bailey JLB, Mayer D, Lohr F, et al. Implementation of a mass canine rabies vaccination campaign in both rural and urban regions in southern Malawi. PLoS Negl Trop Dis. 2020;14(1):e0008004. https://doi.org/10.1371/journal.pntd.0008004 PMID: 31971943.

58. Kaare M, Lembo T, Hampson K, Ernest E, Estes A, Mentzel C, et al. Rabies control in rural Africa: evaluating strategies for effective domestic dog vaccination. Vaccine. 2009;27(1):152–60. https://doi.org/10.1016/j.vaccine.2008.09.054 PMID: 18848595.

59. Sambo M, Hampson K, Changalucha J, Cleaveland S, Lembo T, Lushasi K, et al. Estimating the size of dog populations in Tanzania to inform rabies control. Vet Sci. 2018;5(3):77. https://doi.org/10.3390/vetsci5030077

60. Knobel DL, Cleaveland S, Coleman PG, Fèvre EM, Meltzer MI, Miranda MEG, et al. Re-evaluating the burden of rabies in Africa and Asia. Bull World Health Org. 2005;83(5):360–8. PMID: 15976877.

61. Haydon DT, Randall DA, Matthews L, Knobel DL, Tallents LA, Gravenor MB, et al. Low-coverage vaccination strategies for the conservation of endangered species. Nature. 2006;443(7112):692–5. https://doi.org/10.1038/nature05177 PMID: 17036003.

62. Doherty M, Buchy P, Standaert B, Giaquinto C, Prado-Cohrs D. Vaccine impact: benefits for human health. Vaccine. 2016;34(52):6707–14. https://doi.org/10.1016/j.vaccine.2016.10.025 PMID: 27773475.

63. World Health Organization. Global measles and rubella strategic plan: 2012–2020. 2012, 42.

64. Townsend SE, Lembo T, Cleaveland S, Meslin FX, Miranda ME, Putra AAG, et al. Surveillance guidelines for disease elimination: a case study of canine rabies. Comp Immunol Microbiol Infect Dis. 2013;36(3):249–61. https://doi.org/10.1016/j.cimid.2012.10.008 PMID: 23260376.

65. Beyer HL, Hampson K, Lembo T, Cleaveland S, Kaare M, Haydon DT. Metapopulation dynamics of rabies and the efficacy of vaccination. Proc Biol Sci. 2010;278(1715):2182–90. https://doi.org/10.1098/rspb.2010.2312 PMID: 21159675.

66. Purwo Suseno P, Rysava K, Brum E, De Balogh K, Ketut Diarmita I, Fakhri Husein W, et al. Lessons for rabies control and elimination programmes: a decade of One Health experience from Bali, Indonesia. Rev Sci Tech. 2019;38(1):213–24. https://doi.org/10.20506/rst.38.1.2954 PMID: 31564729.

67. Cooper B. Poxy models and rash decisions. Proc Natl Acad Sci U S A. 2006;103(33):12221–2. https://doi.org/10.1073/pnas.0605502103 PMID: 16894142.

68. Tracy M, Cerdá M, Keyes KM. Agent-based modeling in public health: current applications and future directions. Annu Rev Public Health. 2018;39:77–94. https://doi.org/10.1146/annurev-publhealth-040617-014317 PMID: 29328870.

69. Talbi C, Lemey P, Suchard MA, Abdelatif E, Elharrak M, Nourlil J, et al. Phylodynamics and human-mediated dispersal of a zoonotic virus. PLoS Pathog. 2010;6(10):e1001166. https://doi.org/10.1371/journal.ppat.1001166 PMID: 21060816.

70. Villatoro FJ, Sepúlveda MA, Stowhas P, Silva-Rodríguez EA. Urban dogs in rural areas: Human-mediated movement defines dog populations in southern Chile. Prev Vet Med. 2016;135:59–66. https://doi.org/10.1016/j.prevetmed.2016.11.004 PMID: 27931930.

71. Duamor CT, Hampson K, Lankester F, Lugelo A, Changalucha J, Lushasi KS, et al. Integrating a community-based continuous mass dog vaccination delivery strategy into the veterinary system of Tanzania: a process evaluation using normalization process theory. One Health. 2023;17:100575. https://doi.org/10.1016/j.onehlt.2023.100575 PMID: 37332884.

72. National Bureau of Statistics. The 2012 Population and Housing Census: Village statistics. Tanzania; 2012. Available: https://www.nbs.go.tz/nbs/takwimu/census2012/Village_Statistics(ondoa).pdf.

73. National Bureau of Statistics. The 2022 Population and Housing Census: Administrative units Population Distribution Report. Tanzania; 2022. Available: https://www.nbs.go.tz/nbs/takwimu/Census2022/Administrative_units_Population_Distribution_Report_Tanzania_volume1a.pdf.

74. R Core Team. R: A Language and Environment for Statistical Computing. Vienna, Austria: R Foundation for Statistical Computing; 2022. Available: https://www.R-project.org/.

75. Czupryna AM, Brown JS, Bigambo MA, Whelan CJ, Mehta SD, Santymire RM, et al. Ecology and demography of free-roaming domestic dogs in rural villages near Serengeti National Park in Tanzania. PLoS One. 2016;11(11):e0167092. https://doi.org/10.1371/journal.pone.0167092 PMID: 27893866.

76. Stan Development Team. Stan modeling language users guide and reference manual. 2024. https://mc-stan.org.

77. Stan Development Team. RStan: the R interface to Stan. 2024. Available: https://mc-stan.org/

78. Bürkner P-C. brms: An R Package for Bayesian Multilevel Models Using Stan. J Stat Soft. 2017;80(1). https://doi.org/10.18637/jss.v080.i01

79. Hartig F. DHARMa: Residual Diagnostics for Hierarchical (Multi-Level/ Mixed) Regression Models. 2022. Available: https://CRAN.R-project.org/package=DHARMa

80. Bivand R, Rundel C. rgeos: Interface to Geometry Engine – Open Source ('GEOS'). 2021. Available: https://CRAN.R-project.org/package=rgeos

81. Rajeev M. mrajeev08/treerabid: Zenodo release. Zenodo. 2021 [cited 9 Dec 2023]. https://doi.org/10.5281/zenodo.5269062

82. Delignette-Muller ML, Dutang C. fitdistrplus: AnRPackage for Fitting Distributions. J Stat Soft. 2015;64(4). https://doi.org/10.18637/jss.v064.i04